

AD-A017 403

THE DESIGN OF A PROPELLER FOR A U. S. COAST GUARD  
ICEBREAKER TUGBOAT

R. D. Kader

David W. Taylor Naval Ship Research and Development  
Center

Prepared for:

Coast Guard

October 1975

DISTRIBUTED BY:

**NTIS**

National Technical Information Service  
U. S. DEPARTMENT OF COMMERCE

328165

Report No. SPD-223-19

AD A017403

**DAVID W. TAYLOR**

**NAVAL SHIP RESEARCH AND DEVELOPMENT CENTER**

Bethesda, Maryland 20084



THE DESIGN OF A PROPELLER FOR A U.S. COAST GUARD ICEBREAKER TUGBOAT

by

R.D. Kader

Approved for Public Release;  
Distribution Unlimited

SHIP PERFORMANCE DEPARTMENTAL REPORT

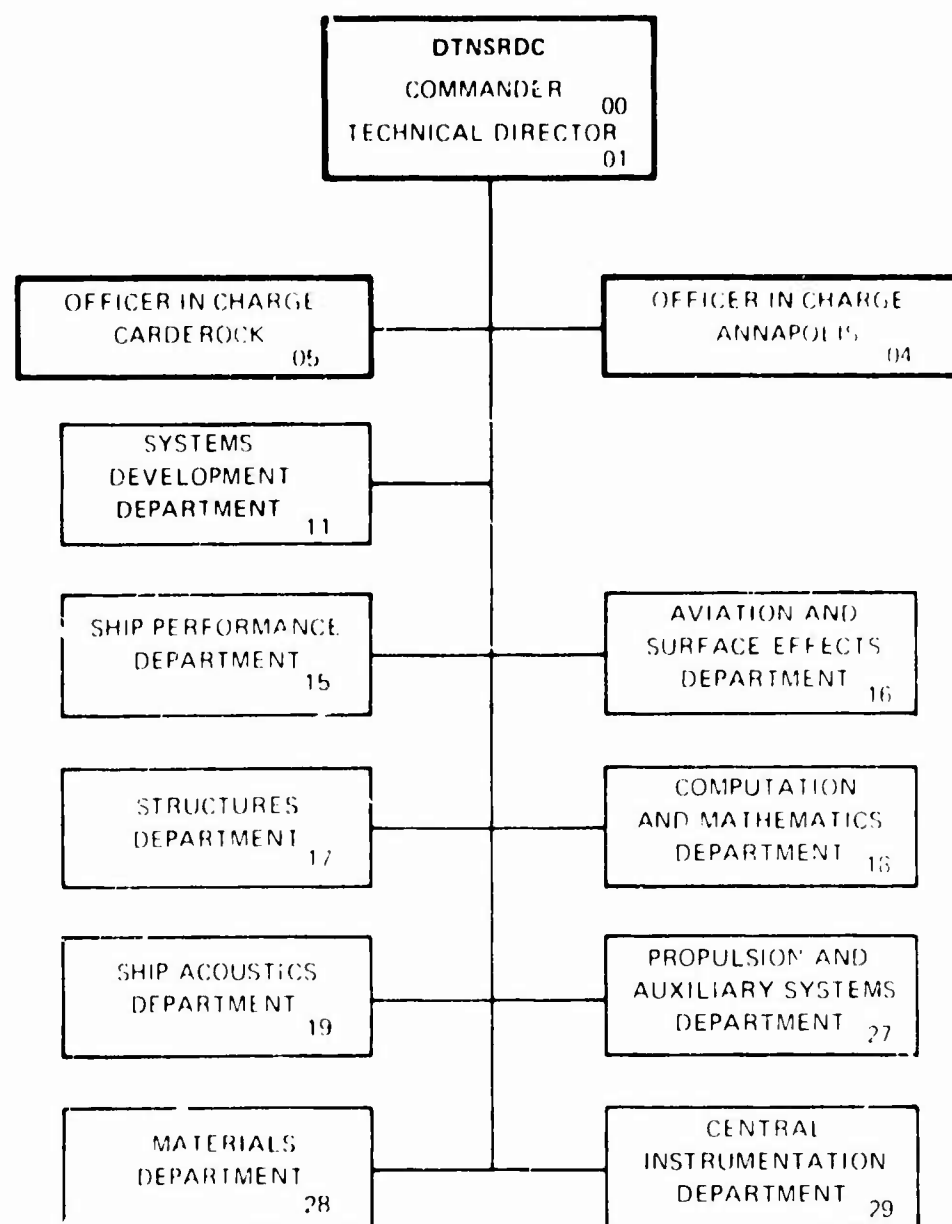
OCTOBER 1975

REPORT NO. SPD-223-19

Reproduced by  
NATIONAL TECHNICAL  
INFORMATION SERVICE

U.S. Department of Commerce  
Springfield, MA 01104

# MAJOR DTNSRDC ORGANIZATIONAL COMPONENTS



"This document contains information affecting the national defense of the United States within the meaning of the Espionage Laws, Title 18, U. S. C., Sections 793 and 794, the transmission or the revelation of its contents in any manner to an unauthorized person is prohibited by law."

A

UNCLASSIFIED

SECURITY CLASSIFICATION OF THIS PAGE (When Data Entered)

REPORT DOCUMENTATION PAGE		READ INSTRUCTIONS BEFORE COMPLETING FORM
1. REPORT NUMBER SPD-223-19	2. GOVT ACCESSION NO.	3. RECIPIENT'S CATALOG NUMBER
4. TITLE (and Subtitle) The Design of a Propeller for a U.S. Coast Guard Icebreaker Tugboat		5. TYPE OF REPORT & PERIOD COVERED Departmental/Final
		6. PERFORMING ORG. REPORT NUMBER
7. AUTHOR(s) R.D. Kader		8. CONTRACT OR GRANT NUMBER(s)
9. PERFORMING ORGANIZATION NAME AND ADDRESS David W. Taylor Naval Ship Research and Development Center		10. PROGRAM ELEMENT, PROJECT, TASK AREA & WORK UNIT NUMBERS
11. CONTROLLING OFFICE NAME AND ADDRESS U.S. Coast Guard 400 Seventh Street, S.W. Washington, D.C. 20591		12. REPORT DATE October 1975
		13. NUMBER OF PAGES 57
14. MONITORING AGENCY NAME & ADDRESS (if different from Controlling Office)		15. SECURITY CLASS (of this report) Unclassified
		15a. DECLASSIFICATION/DOWNGRADING SCHEDULE
16. DISTRIBUTION STATEMENT (of this Report) Approved for Public Release; Distribution Unlimited.		
17. DISTRIBUTION STATEMENT (of the abstract entered in Block 20, if different from Report)		
18. SUPPLEMENTARY NOTES		
19. KEY WORDS (Continue on reverse side if necessary and identify by block number)		
20. ABSTRACT (Continue on reverse side if necessary and identify by block number) The design process for an icebreaker tugboat propeller is presented and considerations involving cavitation, vibratory forces and propeller installation and removal are discussed. The design point for the propeller is maximum thrust at 5 knots full power ahead with pitch selected to give bollard operation at 245 rpm. Good astern thrust at bollard was desired and 75 percent of ahead bollard thrust was provided as a minimum. Preliminary design using series data predicted a propeller with a blade area ratio of 0.70 and a pitch		

DD FORM 1 JAN 73 1473

EDITION OF 1 NOV 65 IS OBSOLETE  
S/N 0102-014-6601

UNCLASSIFIED

SECURITY CLASSIFICATION OF THIS PAGE (When Data Entered)

UNCLASSIFIED

SECURITY CLASSIFICATION OF THIS PAGE (When Data Entered)

ratio of 0.73 would give the highest astern performance at 85 percent of ahead bollard thrust and still fall within the design point restrictions. Intermediate design involved lifting line calculations at the free route condition with a maximum predicted speed of 14.86 knots at full power. Tang $\beta$  distribution was adjusted for reduced-pitch near root to obtain shorter hub length. Lifting surface calculations encompassed the final design phase providing final geometry for a wake adapted design meeting ABS strength requirements.

7

UNCLASSIFIED

SECURITY CLASSIFICATION OF THIS PAGE (When Data Entered)

## TABLE OF CONTENTS

	Page
ABSTRACT. . . . .	1
ADMINISTRATIVE INFORMATION. . . . .	2
INTRODUCTION. . . . .	2
PRELIMINARY TECHNICAL INFORMATION . . . . .	4
PROPELLER DESIGN PROCEDURE. . . . .	5
PRELIMINARY DESIGN. . . . .	6
INTERMEDIATE DESIGN . . . . .	15
FINAL DESIGN. . . . .	18
SUMMARY AND RECOMMENDATIONS . . . . .	24
REFERENCES. . . . .	26

# NOTATION

A	Area of blade section
$A_e$	Expanded area, $\int_{r_h}^R c dr$
$A_0$	Disk area of propeller, $\pi R^2$
c	Section chord length
$c_{0.7}$	Section chord length at 0.7R
D	Propeller diameter
EAR	Expanded area ratio, $A_e/A_0$
$\tilde{F}_H$	Amplitude of blade frequency harmonic of transverse horizontal force
$\tilde{F}_V$	Amplitude of blade frequency harmonic of transverse vertical force
$f_M$	Camber of section
g	Acceleration due to gravity
H	Hydrostatic head at shaft centerline minus vapor head
$H_L$	Hydrostatic head at local position minus vapor head
J	Advance coefficient, $V_A/nD$
$J_L$	Advance coefficient of propeller, local wake, $V_X/[(nD)+(V_T/(\pi r/R))]$
$J_T$	Advance coefficient based on thrust identity
$J_V$	Advance coefficient based on ship speed $V/nD$
$K_Q$	Torque coefficient, $Q/\rho n^2 D^5$
$K_T$	Thrust coefficient, $T/\rho n^2 D^4$
$\tilde{M}_H$	Amplitude of blade frequency harmonic of bending moment about the transverse horizontal axis

$\bar{M}_V$	Amplitude of blade frequency harmonic of bending moment about the vertical axis
$n$	Propeller revolutions per unit time
$(P/D)_I$	Propeller section hydrodynamic pitch ratio, $\pi \tan \beta_I$
$P$	Propeller section pitch
$P_D$	Delivered power at propeller, $2\pi nQ$
$P_E$	Effective power, $RV$
$P_S$	Power delivered to shaft aft of gearing and thrust block
$p$	Local pressure
$p_\infty$	Pressure at infinity
$Q$	Propeller torque
$\bar{Q}$	Amplitude of blade frequency harmonic of torque
$q$	Wake harmonic number
$R$	Propeller radius
$R_n$	Reynolds number for propeller, $c_{0.7} \sqrt{[V_A^2 + (0.7 \pi nD)^2]}/\nu$
$R_F$	Frictional resistance of hull
$R_K$	Local rake offset, positive aft
$R_R$	Residuary resistance of hull
$R_T$	Total resistance of hull
$r$	Radial distance
$r_h$	Radius of hub
$T$	Propeller thrust
$\bar{T}$	Amplitude of blade frequency harmonic of thrust
$t$	Maximum total thickness of blade section



$t$	Thrust deduction fraction, $(T-R_T)/T$
$V$	Ship speed
$V_A$	Speed of advance of propeller, $V(1-w_T)$
$w_Q$	Taylor wake fraction determined from torque identity
$w_T$	Taylor wake fraction determined from thrust identity
$w_x$	Local wake fraction
$x$	Nondimensional radial distance, $r/R$
$Z$	Number of blades
$\eta_P$	Propulsive efficiency, $P_E/P_D$
$\eta_H$	Hull efficiency, $(1-t)/(1-w_T)$
$\eta_O$	Propeller efficiency in open water
$\eta_R$	Relative rotative efficiency
$\eta_S$	Propulsive efficiency, $P_E/P_S$
$\rho$	Mass density of water
$\rho_P$	Mass density of propeller
$\nu$	Kinematic viscosity
$\sigma$	Cavitation number based on vapor pressure, $2gH/V^2$

## LIST OF FIGURES

	Page
Figure 1 - Series Prediction for an 8.5-foot Diameter Propeller Absorbing Full Power at Five Knots Ahead . . . . .	27
Figure 2 - Prediction of Astern Bollard Thrust to Ahead Bollard Thrust Ratio and Actual Astern Bollard Thrust . . . . .	28
Figure 3 - Series Prediction for Full Power Five Knots Ahead Condition for a 7.5-foot Diameter Propeller. . . . .	29
Figure 4 - Prediction of Occurrence of Thrust Breakdown . . . . .	30
Figure 5 - Self Propulsion Performance of Model 5336 Fitted with Stock Propeller. . . . .	31
Figure 6 - Series Prediction of Full Power Free Route RPM and Velocity. . . . .	32
Figure 7 - Wake Survey Velocity Component Ratios at Experimental Radii . . . . .	33
Figure 8 - Hull Lines of Model 5336. . . . .	38
Figure 9 - Radial Distribution of Thickness. . . . .	39
Figure 10 - Radial Distribution of Chord Length . . . .	40
Figure 11 - Final Pitch Distribution . . . . .	41
Figure 12 - Final Camber Distribution . . . . .	42
Figure 13 - Limits of Cavitation and Hull-Transmitted Propeller Vibration . . . . .	43

# LIST OF TABLES

	Page
Table 1 - Self Propulsion Performance of Model 5336 Fitted with Stock Propeller - Channel Results. . . . .	44
Table 2 - Wake Survey Analysis for Model 5336. . . . .	45
Table 3 - Stress Levels from Intermediate Design Phase. . . . .	46
Table 4 - Geometric Characteristics of Propeller . . .	47
Table 5 - Amplitude of Blade Frequency Forces and Moments for Final Design . . . . .	48

## ABSTRACT

The design process for an icebreaker tugboat propeller is presented and considerations involving cavitation, vibratory forces and propeller installation and removal are discussed. The design point for the propeller is maximum thrust at 5 knots full power ahead with pitch selected to give bollard operation at 245 rpm. Good astern thrust at bollard was desired and 75 percent of ahead bollard thrust was provided as a minimum. Preliminary design using series data predicted a propeller with a blade area ratio of 0.70 and a pitch ratio of 0.73 would give the highest astern performance at 85 percent of ahead bollard thrust and still fall within the design point restrictions. Intermediate design involved lifting line calculations at the free route condition with a maximum predicted speed of 14.86 knots at full power.  $\tan \epsilon_i$  distribution was adjusted for reduced-pitch near root to obtain shorter hub length. Lifting surface calculations encompassed the final design phase providing final geometry for a wake adapted design meeting ABS strength requirements.

## ADMINISTRATIVE INFORMATION

This work was performed at the Naval Ship Research and Development Center under authorization by the U.S. Coast Guard under increased funding to MIPR Z 70099-4-44131, 27 June 1974. This work was performed under the NSRDC Work Unit 1524-550.

## INTRODUCTION

The design of tug propellers is a complicated process in that the operating conditions vary over a wide range and there is a difference in power characteristics between the propeller and the engine. The operating conditions for a tug vary from the static condition at bollard, low speed towing and finally to the free-running condition. At each of these conditions the available full power of the engine is used which necessitates some trade-offs in the design since a fixed pitch propeller will only absorb this power at one rpm and one advance velocity. Normal practice is to design a propeller for the full power, free route condition enabling a lifting line calculation procedure to be used. Unfortunately, the design point for tug propellers is most often the low speed towing condition which dictates a change in the design procedure.

Any of the three operating conditions can be chosen for the design point. However, each choice will result in a loss at the other two conditions and in this particular design the bollard rpm is reduced and the maximum advance velocity at the free route condition is not obtained. The altered design procedure for a tug propeller involves the use of series data to determine the best propeller to meet the design conditions. This best choice is then checked against performance requirements at bollard and lifting line calculations are made at the free route condition. The series data choice provides the additional information to check the propeller at the bollard and free running condition.

This design is further complicated by the fact that the tugboat will also experience duty as an icebreaker. The presence of ice in the operating region has its greatest influence upon propeller rpm in that rpm is reduced when the blades operate in a heavier two phase mixture of ice and water, crash into a large block of ice or when ice wedges between the blade tips and the hull. This reduction of rpm will manifest itself as a loss in thrust at all operating conditions.

#### PRELIMINARY TECHNICAL INFORMATION

The U.S. Coast Guard provided design conditions and guidelines for the propeller design as follows:

Diameter	8.5 feet
Number of blades	4
Shaft horsepower	2500 DC/DC Electric
Full power free route rpm	305
Full power bollard rpm	245
Rotation	RH
Material	Ni-Al-Br ABS Alloy 4
Hub diameter	25 percent of propeller diameter

NOTE: The full power of the engine is available at any speed between bollard and free route in the limits of rpm between 245 and 305.

In addition, certain design requirements and performance were specified as follows:

1. Strength requirements shall be in accordance with section 29, Part II of the "ABS Rules for Building and Classing Steel Vessels", ice class IAA, 1972.
2. The astern bollard thrust at 2500 SHP shall be approximately 75 percent of ahead bollard thrust.

3. The design point shall be maximum thrust at full power and 5 knots ahead. The propeller pitch must be selected to allow full power bollard operation at 245 rpm.

#### PROPELLER DESIGN PROCEDURE

Basically the propeller was designed in three phases:

1. Preliminary Design: Preliminary design analysis was conducted using series data to determine the effect of pitch, diameter and blade area on performance at the design point and also at bollard and free route. Blade area and pitch are selected for input to next phase and thickness chosen to meet ABS strength requirements. The occurrence and severity of cavitation will be examined.

2. Intermediate Design: Lifting line calculations are performed at the free route condition to obtain maximum speed, stress levels and inputs for next phase. Wake fraction and  $\tan\delta_i$  distributions are adjusted for comparison of final pitch to preliminary design pitch and reduce the overall hub length.

3. Final Design: Lifting surface calculations are performed to determine the final propeller geometry. Rake was chosen to increase the tip clearance between propeller and stern. Section shape and meanline was chosen to meet desired performance.



## PRELIMINARY DESIGN

Common practice has dictated the design point for a tugboat propeller to be maximum thrust in the bollard condition or at some low intermediate speed since a tugboat very seldom operates at the free running condition. Normally, standard propeller series data is used for the hydrodynamic design with no consideration given for the presence of solid ice pieces in the operating area for designs seeing duty as icebreakers. The series data used as a basis in this design is the Troost  $B_4$  series as investigated by Van Lammeren, Van Manen, and Oosterveld<sup>1</sup>. This propeller series, commonly referred to as the Wageningen B-screw series, comprise models with systematically varying P/D ratios and blade area ratio  $A_E/A_0$  with performance presented as open water curves over an entire region of operation.

The first step in the preliminary design phase is satisfying the condition of optimum thrust at full power and 5 knots ahead which is the design point. The only known quantities at this condition are propeller diameter (8.5 feet), shaft horsepower (2500), and ship speed (5 knots). The advance coefficient, J, must be known

---

1. VanLammeren, W.P.A., VanManen, J.D., and Oosterveld, M.W.C., "The Wageningen B-Screw Series," Transactions of the Society of Naval Architects and Marine Engineers, Vol. 77, p 269-317, 1969

to use the series data, so some value of rpm is chosen. The technical guidelines provide a range of rpm, 245-305, to work within and the actual rpm at the towing condition will be somewhat higher than the 245 bollard rpm. Therefore, a range of propeller rpm is chosen, in this case 250-310, and the corresponding advance coefficient  $J$  and torque coefficient  $K_Q$  are evaluated at each rpm chosen within the range. The advance coefficient by which the series data is plotted uses the speed of advance of the propeller not the ship speed. Therefore, the ship speed (5 knots) must be adjusted by the appropriate wake fraction at this operating condition which can be found from previous propulsion experiments provided in Reference 2 and Table 1. The pitch ratio,  $P/D$ , specified by  $J$  and  $K_Q$  is obtained from series data for various values of blade area. The thrust coefficient  $K_T$  and actual thrust is specified by the pitch and advance coefficient. The maximum thrust for each blade area ratio examined is found by plotting thrust versus  $P/D$  and the results are presented in Figure 1. Each data point on the curves represented by symbols is a choice of rpm within the range, in this

2. West, E.E., "Powering Predictions for the United States Coast Guard 140-Foot WYTM Represented by Model 5336," Ship Performance Department Report SPD-223-16, April 1975

case an increment of 10 was chosen beginning with 250. The figure shows that thrust decreases with increasing blade area following along a line of constant pitch. It is also noted that the pitch which delivers maximum thrust increases as the blade area increases.

The appropriate P/D ratio to allow 245 rpm at the full power bollard condition can be determined by using the value of the torque coefficient at  $J=0$ . The value of the bollard  $K_Q$ , in this case 0.0364, specified by SHP and rpm, provides the P/D to absorb this torque for each blade area examined. This curve is also provided on Figure 1. The design requirements dictate that the final design point for this propeller must fall on this curve, assuming cavitation free operation. To avoid confusion it is pointed out that the values of thrust along this curve are irrelevant since they were calculated for the 5 knot condition and not bollard operation. It is also noted that as the blade area is increased the pitch to deliver 254 bollard rpm and the pitch for maximum thrust get closer together.

To locate the approximate final design point on the 245 bollard rpm curve in Figure 1, the requirement of at least 75 percent astern bollard thrust compared to

ahead bollard thrust is used. Unfortunately, only a limited amount of four quadrant open water data for series propellers is available. Reference 1 provides experimental four quadrant open water results for selected propellers of the Wageningen B-Series and a regression analysis was performed to provide Fourier coefficients to predict performance for different blade area and pitch ratios. A computerized prediction technique has been developed by Strom-Tejsen and Porter<sup>3</sup> using experimental data reported by Miniovich<sup>4</sup>. This computer program is capable of predicting four quadrant open-water performance for propellers with a blade area ratio between 0.45 and 0.85 and a pitch ratio from -1.1 to 1.6. The above techniques are used to predict the astern performance for this propeller and the results are presented in Figure . The experimental results upon which the prediction techniques are based assume an astern thrust deduction of 0. However, previous propulsion experiments, found in Reference 2, using a stock propeller gave an ahead bollard tow rope pull approximately equal to 100 percent of propeller thrust and an astern tow

3. Strom-Tejsen, J. and Porter, R.R., "Prediction of Controllable-Pitch Propeller Performance in Off-Design Conditions," Paper presented at the Third Ship Control Systems Symposium at Bath, England, August 1972
4. Miniovich, I.Y., "Investigation of Hydrodynamic Characteristics of Screw Propellers Under Conditions of Reversing and Calculation Methods for Backing of Ships," Transactions of the A.N.Krylov Research Institute, Issue 122, 1958; (English Translation: Bureau of Ships Translation 697, Washington, D.C., 1960)

rope pull equal to 83 percent of propeller thrust. This value of 83 percent for the astern bollard thrust deduction has already been incorporated in the results presented in Figure 2. The curve for  $P/D=1.0$  over a range of blade area and the single point at  $P/D=1.4$  and  $EAR=0.70$  provide noticable trends over a range of blade area and pitch. These points are the only ones presented since they were experimentally determined. The computer prediction of Reference 3 was used for the tentative design geometry and this is also provided on Figure 2. The trends presented indicate that the percentage of astern thrust to ahead thrust reaches a maximum at an area ratio of 0.70 and along a constant blade area line the percentage increases continuously with decreasing pitch. Since the delivered thrust increases with decreasing blade area the actual astern thrust may not follow the curve in Figure 2. For a pitch ratio of 1.0 the actual astern thrust was determined over a range of blade area and this is also provided in Figure 2. It is seen that increasing the blade area past 0.70 gives no appreciable increase in astern thrust. Therefore, the tentative final design point to be carried on to the next phase

is chosen as  $EAR=0.70$  and  $P/D=0.73$ . No considerations as to the effects of cavitation and thrust breakdown have been incorporated in making this choice but will be discussed later.

Enkvist and Johansson<sup>5</sup> determined that propellers with higher pitch ratios and smaller diameter have shown to produce more thrust in ice than propellers which give optimum bollard thrust in ice-free water. The advantages of a smaller diameter propeller are the greater tip clearance to prevent pieces of ice from wedging between the propeller tip and the hull and in submergence effects, specifically, cavitation and possible air drawing. As an aside to investigate the possible benefits of a smaller diameter for this design the first step described previously was carried out for a diameter of 7.5 feet. These results are presented in Figure 3. The figure indicates that the maximum thrust does not occur within the  $P/D$  range examined for most blade area ratios and the decrease in diameter would precipitate a reduction in thrust of around 10 percent as compared to an 8.5-foot diameter. The pitch ratio to give 245 bollard rpm is also too high to meet the astern thrust requirements. It is, therefore, concluded that an 8.5-foot diameter propeller is the better choice.

---

5. Enkvist, E. and Johansson, B.M., "On Icebreaker Screw Design," European Shipbuilding No. 1, p 2-14, p18-19, 1968

Due to the rugged operating conditions and the absence of skew, normal propeller designs use a Troost blade outline adjusted to meet any specific needs. For this design the 4-bladed Troost 0.7 blade area ratio outline was used and adjusted to maintain the same blade area for the 25 percent hub diameter recommended by the U.S. Coast Guard. ABS rules for icebreaker propellers provide minimum values for the section modulus at the 0.25 and 0.6 radial stations and also the minimum tip thickness. The thickness at any radial station can be determined from the section modulus divided by the chord length. The chord length and thickness are necessary inputs to the second phase of the design.

The effect of cavitation on propeller performance can manifest itself as a loss in thrust commonly referred to as thrust breakdown. Thrust breakdown at the bollard condition is especially critical for this design. Enkvist and Johansson<sup>5</sup> compiled data on many propellers operating at the bollard condition and provide a prediction for the occurrence of thrust breakdown for this propeller design. Their results have been reduced to eliminate extraneous data and are presented in Figure 4. These

results indicate the tentative design is inside the no thrust breakdown region. Prishchemikim<sup>6</sup> has also reported the extent of breakdown as a function of rotational cavitation number,  $\sigma_n$ , at the bollard condition. His results were reported for a B4-55 propeller and were crudely extrapolated to an area ratio of 0.70. Since the curve for the higher blade area was roughly approximated it has not been included for presentation. The rotational cavitation number at the bollard condition for this propeller is equal to 1.9 and according to Reference 6 the loss in thrust and torque at this value of  $\sigma_n$  will amount to less than 5 percent. Obviously the above predictions are in complete disagreement and supports the need for further experimentation and the instability of cavitation phenomena.

Another detrimental effect on thrust is the phenomena of air drawing which occurs when the propeller sucks air down from the free surface of the water forming a vortex

---

6. Prishchemikin, Y.N., "A Study of the Cavitating Propeller and Ship Hull Interaction in Cavitation Towing Tank," 14th International Towing Tank Conference, 1975



from the free surface to the blade surface. This condition will occur only at the bollard condition or very low speed which is the primary operating range for a tugboat. The presence of air drawing will result in a drop in efficiency of the propeller, but more seriously will cause instability and sudden increases in propeller revolutions and consequently sudden change in thrust and torque which could cause damage to the main engine. The only extensive investigation of air drawing has been reported by Shiba<sup>7</sup> for propellers not completely immersed and at shallow immersion. These results were crudely extrapolated for extension to the immersion depth of this design. The extent of air drawing can be approximated using the so-called Froude number and Weber number. The propeller Froude number ( $n\sqrt{P/g}$ ) decides the maximum depth to which air is sucked down into the propeller disc. As the Froude number increases the depth of air drawing increases and the thrust decreases. The scale effect due to Froude number normally disappears after a value of 3. The Froude number at bollard for this propeller is equal to 2.1. If air drawing has set in then the propeller will be working under the influence of the

---

7. Shiba, H., "Air Drawing of Marine Propellers," Report of the Transportation Technical Research Institute No. 9, August 1953

Froude number. The Weber number ( $nD\sqrt{\rho/50}$ ) is a measure of the suction force to overcome the water surface tension and draw air down to the propeller. The influence of the Weber number generally disappears at values higher than 180. The Weber number at bollard for this propeller is 2012 so it will be working outside the range of Weber number influence. Unfortunately, model experiments generally operate within the range of Weber number influence. Flow visualization studies using the stock propeller have shown intermittent air drawing. The occurrence of air drawing for this design cannot be concretely predicted and neither can the chances be diminished by adjusting the blade area and pitch since design requirements rule out any of these changes.

All preliminary groundwork has now been completed for this design and it is ready to enter into the intermediate phase.

#### INTERMEDIATE DESIGN

The intermediate design phase for this propeller involves a lifting line calculation for the free-route, full power condition. This condition is chosen over the

actual design point because self propulsion experiments for this design did not provide all the necessary inputs for the towing condition. All the necessary data to perform a lifting line calculation for the free-route condition are known except rpm. The 305 rpm specified in the design condition is the free route rpm but may not be equivalent to series prediction which has been the method used so far in this design. To determine the series data rpm prediction, a ship curve,  $K_T/J^2$ , is plotted on the open-water curves for the range of blade area examined. In this case the value of  $K_T/J^2=0.7$  is used because it corresponds approximately to the value obtained in previous propulsion experiments with the results reproduced in Table 1 and Figure 5. For each  $J$  and  $K_T$  the appropriate  $P/D$  can be obtained and also the corresponding  $K_Q$ . The rpm for the full power condition can be determined from this value of  $K_Q$ . The results of this calculation are presented in Figure 6. The speed of advance and also the ship speed can be predicted from the rpm and advance coefficient. This is also provided in Figure 6. Confidence in the method of design using series data can be derived by comparing the series data prediction of ship speed and the lifting line prediction. The closer the two are, the better the method of design looks. For the design point arrived at in phase

1 of  $EAR=0.70$  and  $P/D=0.73$  the series data prediction of rpm is 299 and a ship speed of 14.90 knots. The value of rpm is below the design condition of 305 but the slight decrease was acceptable to the U.S. Coast Guard. Trends shown in the figure indicate that the rpm and ship speed both decrease for increasing blade area with rpm decreasing almost linearly with increasing pitch. The maximum velocity will occur at a higher  $P/D$  ratio as the blade area is increased. At 305 rpm the predicted speed is less than the maximum attainable speed as is 299 rpm.

All data is now known for a first lifting line calculation. The first run through will provide a Lerbs optimum for the  $\tan\beta_i$  distribution. The lifting line prediction for ship speed is 14.83 knots which is in good agreement with the series data prediction and therefore, the design method using series data is considered good. The wake survey used is presented in Figure 7 and Table 2. The predicted stress levels are provided in Table 3.

During this phase of the design the U.S. Coast Guard requested an investigation into reducing the overall hub length to facilitate the installation and removal of the propeller without having to remove the rudder. This reduction in hub length was accomplished by reducing the pitch near the hub and thereby reducing

$\tan\beta$ , near the hub. A subsequent lifting line calculation was performed with a reduction in the radial loading from the 0.6 radius to the hub. The predicted ship speed has risen slightly to 14.86 knots and is even closer to the series data prediction.

The second phase of the propeller design is now complete with all necessary data known to go on to phase 3.

#### FINAL DESIGN

The final design phase for this propeller consists of a lifting surface calculation to determine the final geometry. The final theoretical camber and pitch distributions were determined using the lifting surface procedure of Kerwin<sup>8</sup>.

Subsequent to the start of this propeller design the location of the propeller on the ship was moved forward. The ship lines are presented in Figure 8. Moving the propeller closer to the hull reduces the tip clearance and the chances increase that a piece of ice will become lodged between the propeller tip and the hull. To maintain the same tip clearance as was available in the initial propeller location, a tip rake amounting to 13 degrees from the shaft centerline would be needed. This

---

8. Kerwin, J.E., "Computer Techniques for Propeller Blade Section Design," Proceedings of the Second Lips Propeller Symposium, Drunen, Holland, p 7-31, May 1973

value is somewhat high since the propeller tip would extend past the aft end of the hub so a lower value of 8 degrees with a linear distribution was chosen. This lower value of rake results in a loss in tip clearance of 15 percent from the original propeller location but since the original tip clearance was quite generous this loss was not considered excessive.

The lifting surface procedure of Kerwin<sup>8</sup> does consider the influence of rake. The initial lifting surface pitch distribution is then used for a final thickness check to meet ABS rules and a subsequent lifting surface calculation is performed with the adjusted thickness. The final thickness distribution is contained in Figure 9 and the final chord length distribution is presented in Figure 10. The final pitch distribution is presented in Figure 11. Included in Figure 11 is the Troost pitch curve for  $P/D=0.73$  and a comparison shows the effect of a wake adapted design and the hub length restriction. The final camber distribution is presented in Figure 12 with certain irregularities smoothed out. These irregularities consisted of waviness in the camber curve around mid-span and it was thought that this slight waviness may cause kinks in the blade surface which are not too desirable. Complete propeller geometry is provided in Table 4.

The choice of section shape and meanline was based upon the performance requirements. The meanline chosen for this design is the NACA 65 elliptical meanline and the elliptical distribution was chosen as the section shape which is elliptical from the leading edge to midchord and a fourth degree polynomial or parabolic aft of the midchord.

A last investigation in this phase of the design is the extent of propeller associated vibration. Propeller associated vibration arises from two sources: 1) the unsteady bearing forces which are associated with the propeller blade operating in a spatially varying wake field and unsteady forces being introduced through the shaft, and 2) the pressure forces which are associated with the rotation of the propeller past the hull.

The unsteady bearing forces and resulting moments have been theoretically evaluated for this design using a computerized technique developed by Tsakonas<sup>9</sup>. The predictions are contained in Table 4. Past investigations have indicated an unskewed propeller will exhibit high

---

9. Tsakonas, S., Breslin, J., and Miller, M.L., "Correlation and Application of an Unsteady Flow Theory for Propeller Forces," Transactions of the Society of Naval Architects and Marine Engineers, Vol. 75, p 158-193, 1967

unsteady forces and 3 percent of the mean thrust for the unsteady thrust amplitude for this design is considered high when compared to a ship like the OBO as reported by Valentine<sup>10</sup>. The addition of blade skew angle has shown to be beneficial in reducing these forces, but the use of a significant amount of skew angle in this design is not recommended due to reduced astern thrust and the increased probability of blade damage when the propeller is rotating in the astern direction in the presence of ice. As the propeller rotates the thrust developed by one blade is not constant but fluctuates as the blade sees the different velocities in the wake. These fluctuating forces set up a vibration in the propeller which can be transmitted through the shaft to the hull and on to the power machinery. If the frequency of these fluctuating forces is equal to a resonant frequency of the hull, severe vibration problems will arise. Fortunately, icebreaker hull requirements demand thick hull plating and

---

10. Valentine, D.T. and Dashnaw, F.J., "Highly Skewed Propeller for San Clemente Ore/Bulk/Oil Carrier - Design Considerations Model and Full-Scale Evaluation," Society of Naval Architects and Marine Engineers STAR Symposium, Washington, D.C., August 1975



therefore, the higher unsteady forces may not cause local hull vibration problems. The unsteady force caused vibration transmitted to the machinery cannot be accurately predicted without a vibratory response analysis of the main propulsion machinery system.

The second source of vibration problems arise from unsteady pressures induced by the rotating propeller on nearby portions of the hull and appendages. These pressure forces are most dependent upon the clearance between the ship hull and the propeller, the blade thickness and the blade loading. It has been assumed that the peak pressures near a propeller vary as the distance squared of the tip clearance. The incorporation of rake in this design has made the clearance still quite generous which would tend to decrease the effect of pressure related unsteady forces. Thicker blade sections have an increasing effect on pressure forces and unfortunately ABS rules have dictated thick sections for the design and this may cancel out any improvements obtained through increasing the tip clearance. A symmetrical blade loading

pattern as is incorporated in this design on the other hand tends to decrease the pressure force. Therefore, this design has one plus and two minuses in terms of unsteady pressure forces and a rough guess would say the effect of unsteady pressure forces is low. A systematic investigation into propeller-induced vibrations associated with hull-pressure forces has been reported by Van Gunsteren and Pronk<sup>11</sup>. They investigated both single and twin screw ships of various types and the results are reproduced in Figure 13. The present design has been included in this figure and falls outside the area where severe vibration problems would be expected to be encountered.

---

11. VanGunsteren, L.A. and Pronk, C., "Propeller Design Concepts," Proceedings of the Second Lips Propeller Symposium, Drunen, Holland, P 35-38, May 1973

## SUMMARY AND RECOMMENDATIONS

Series data predicted a propeller with a blade area ratio of 0.70 and a pitch ratio of 0.73 will have the best overall performance when considering all operating points and design requirements. The final design has a wake-adapted pitch distribution with a reduction at the hub to obtain the shortest possible hub length. The hub length was reduced to facilitate propeller installation and removal. During the final ship design, the propeller was moved forward, closer to the hull. A rake of 8 degrees, from the shaft centerline, was added to the propeller to increase the clearance between the propeller and the hull. Predicted astern operation at the bollard condition of 85 percent will exceed the design requirements. Cavitation of sufficient severity to cause thrust breakdown cannot be accurately predicted but should only occur at the bollard condition if at all. The occurrence of air drawing and its detrimental effects also cannot be accurately predicted for this design. Stress levels are low due to ABS requirements for section modulus. Unsteady forces which can cause vibration are relatively higher compared to propeller designed for reduced vibration, but without further detailed studies the potential for serious vibration problems cannot be accurately assessed.

It is recommended that the full scale propeller be built as designed. It is also recommended that a model be built and cavitation performance at the bollard condition be examined to determine the extent of thrust breakdown.

## REFERENCES

1. Van Lammeren, W.P.A., Van Manen, J.D., and Oosterveld, M.W.C., "The Wageningen B-Screw Series," Transactions of the Society of Naval Architects and Marine Engineers, Vol. 77, p 269-317, 1969
2. West, E.E., "Powering Predictions for the United States Coast Guard 140-Foot WYTM Represented by Model 5336," Ship Performance Department Report SPD-223-16, April 1975
3. Strom-Tejsen, J. and Porter, R.R., "Prediction of Controllable-Pitch Propeller Performance in Off-Design Conditions," Paper presented at the Third Ship Control Systems Symposium at Bath, England, August 1972
4. Miniovich, I.Y., "Investigation of Hydrodynamic Characteristics of Screw Propellers Under Conditions of Reversing and Calculation Methods for Backing of Ships," Transactions of the A.N.Krylov Research Institute, Issue 122, 1958; (English Translation: Bureau of Ships Translation 697, Washington, D.C., 1960)
5. Enkvist, E. and Johansson, B.M., "On Icebreaker Screw Design," European Shipbuilding No. 1, p 2-14, p18-19, 1968
6. Prishchemikin, Y.N., "A Study of the Cavitating Propeller and Ship Hull Interaction in Cavitation Towing Tank," 14th International Towing Tank Conference, 1975
7. Shiba, H., "Air Drawing of Marine Propellers," Report of the Transportation Technical Research Institute No. 9, August 1953
8. Kerwin, J.E., "Computer Techniques for Propeller Blade Section Design," Proceedings of the Second Lips Propeller Symposium, Drunen, Holland, p 7-31, May 1973
9. Tsakonas, S., Breslin, J., and Miller, M.L., "Correlation and Application of an Unsteady Flow Theory for Propeller Forces," Transactions of the Society of Naval Architects and Marine Engineers, Vol. 75, p 158-193, 1967
10. Valentine, D.T. and Dashnaw, F.J., "Highly Skewed Propeller for San Clemente Ore/Bulk/Oil Carrier - Design Considerations Model and Full-Scale Evaluation," Society of Naval Architects and Marine Engineers STAR Symposium, Washington, D.C., August 1975
11. Van Gunsteren, L.A. and Pronk, C., "Propeller Design Concepts," Proceedings of the Second Lips Propeller Symposium, Drunen, Holland, P 35-38, May 1973

Figure 1 - Series Prediction for an 8.5-Foot Diameter Propeller  
Absorbing Full Power at Five Knots Ahead

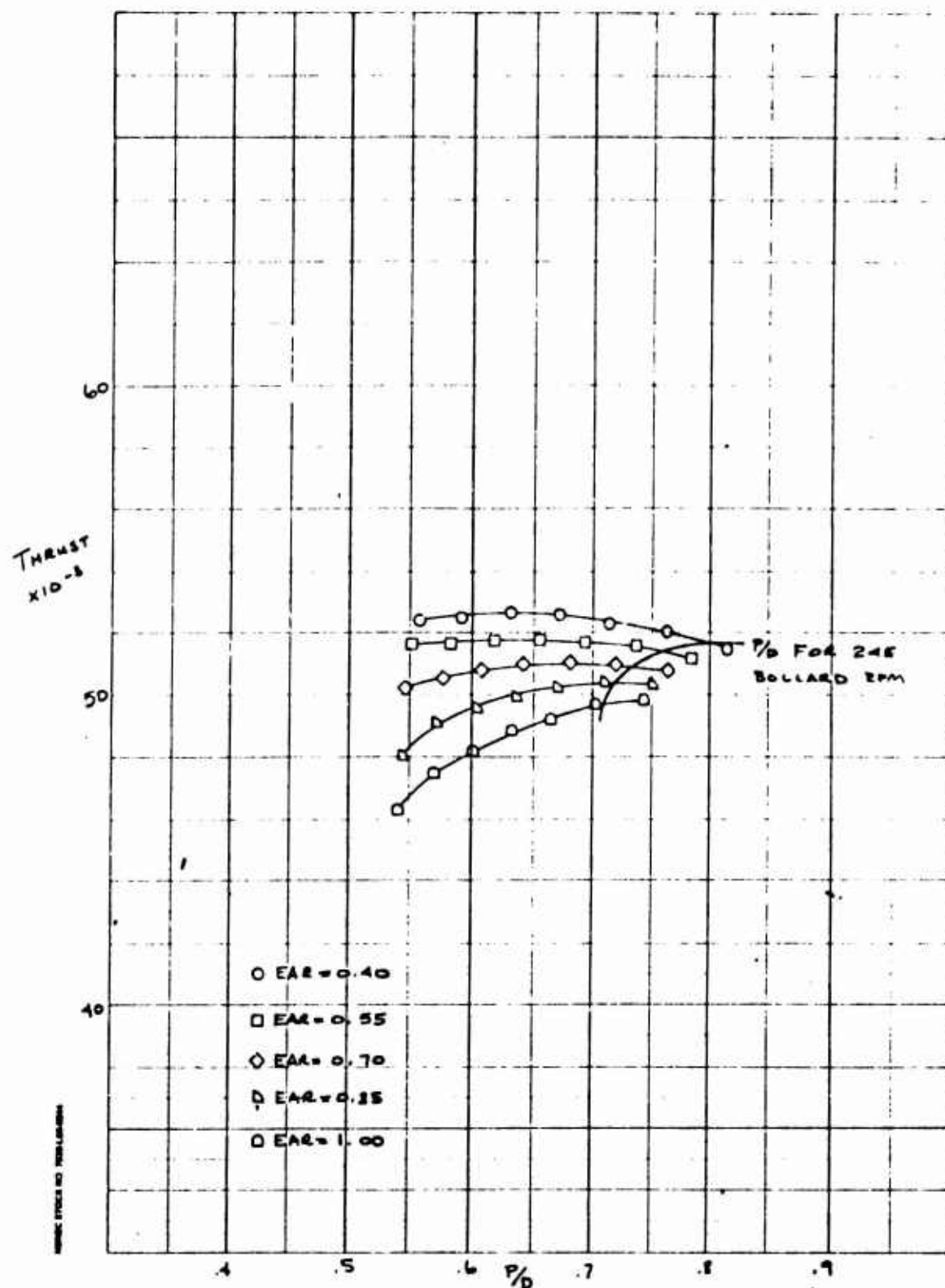


Figure 2 - Prediction of Astern Bollard Thrust to Ahead Bollard Thrust Ratio and Actual Astern Bollard Thrust

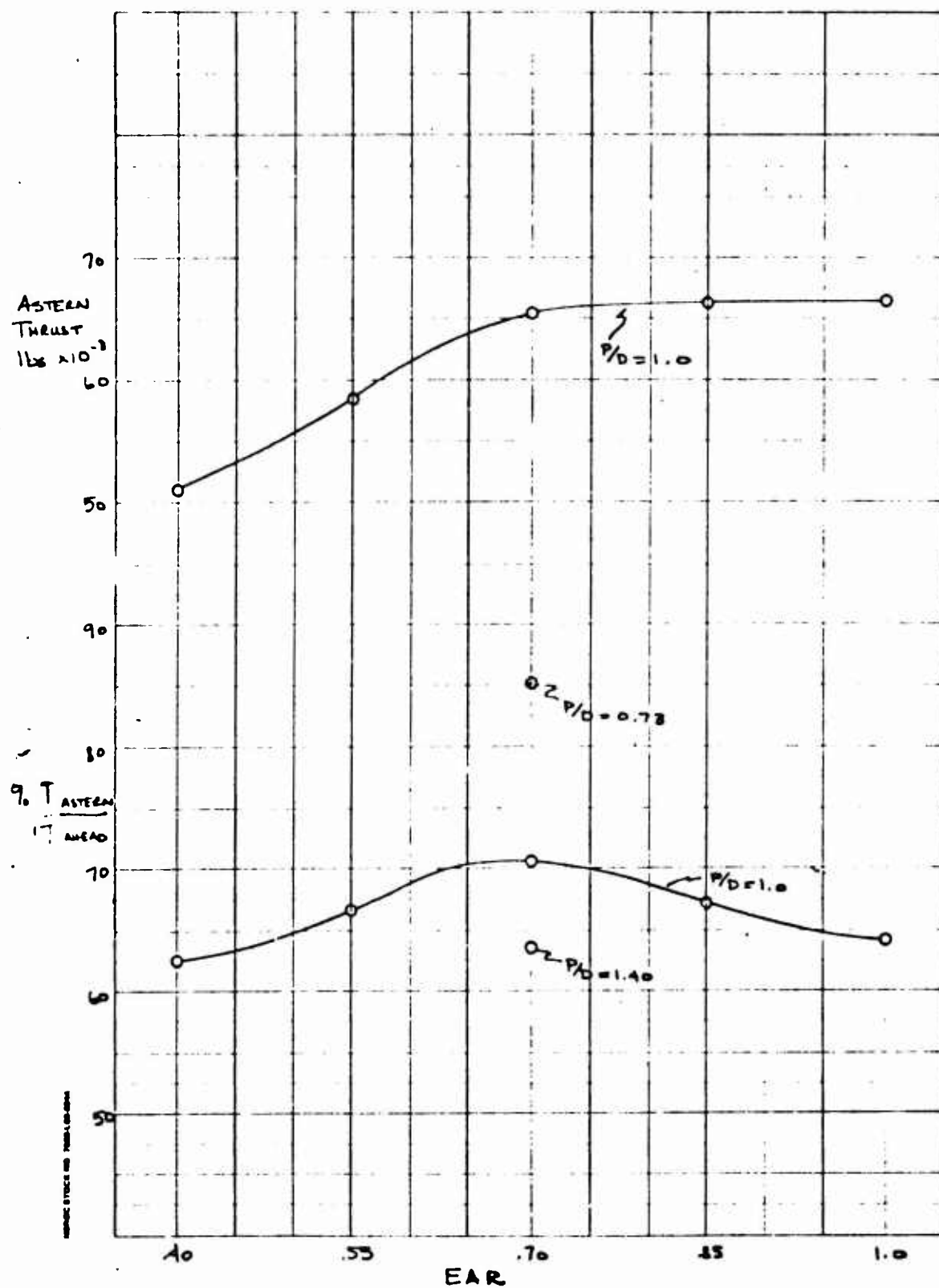


Figure 3 - Series Prediction for Full Power Five Knots Ahead  
Condition for a 7.5-Foot Diameter Propeller

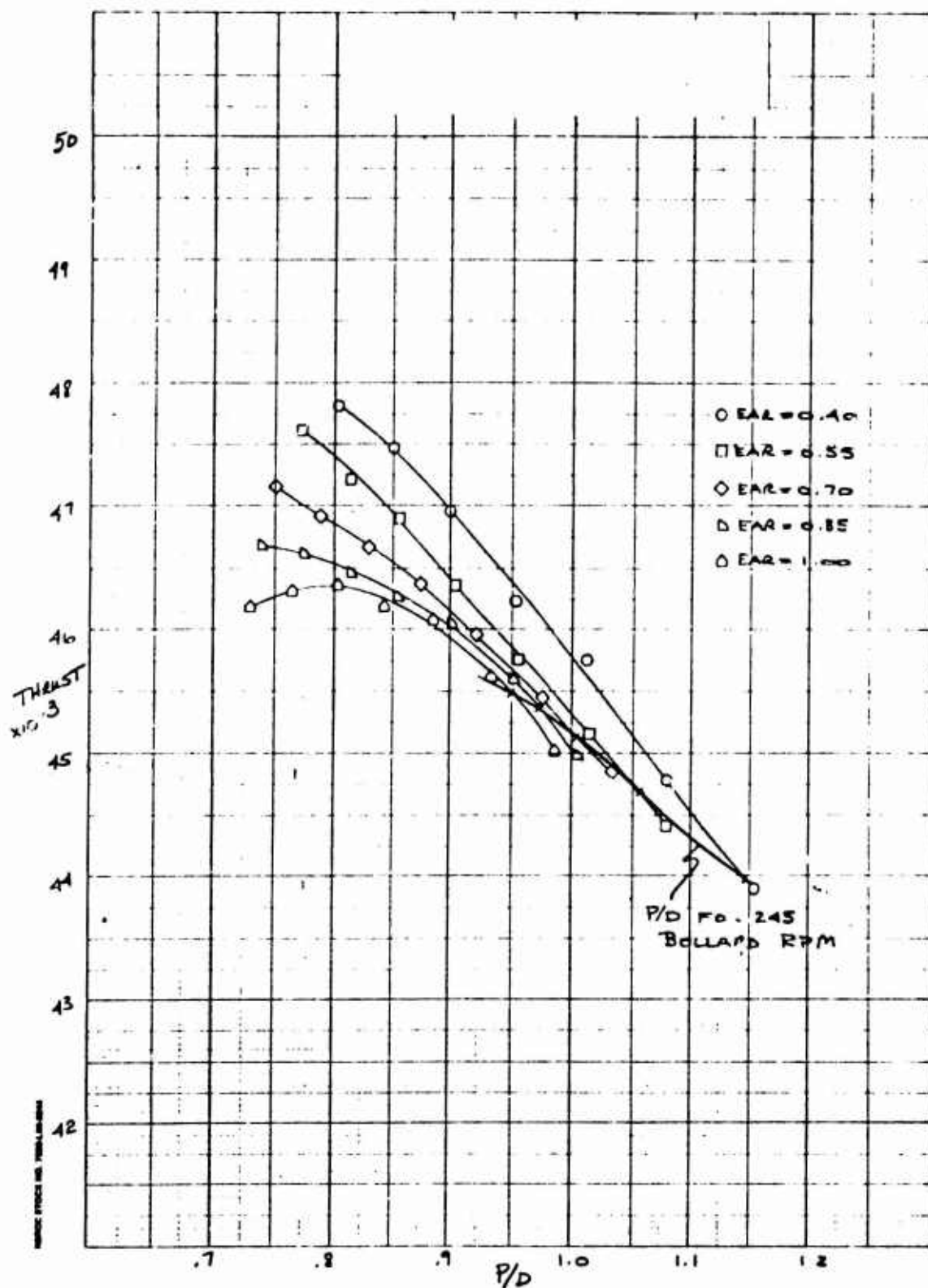




Figure 4 - Prediction of Occurrence of Thrust Breakdown

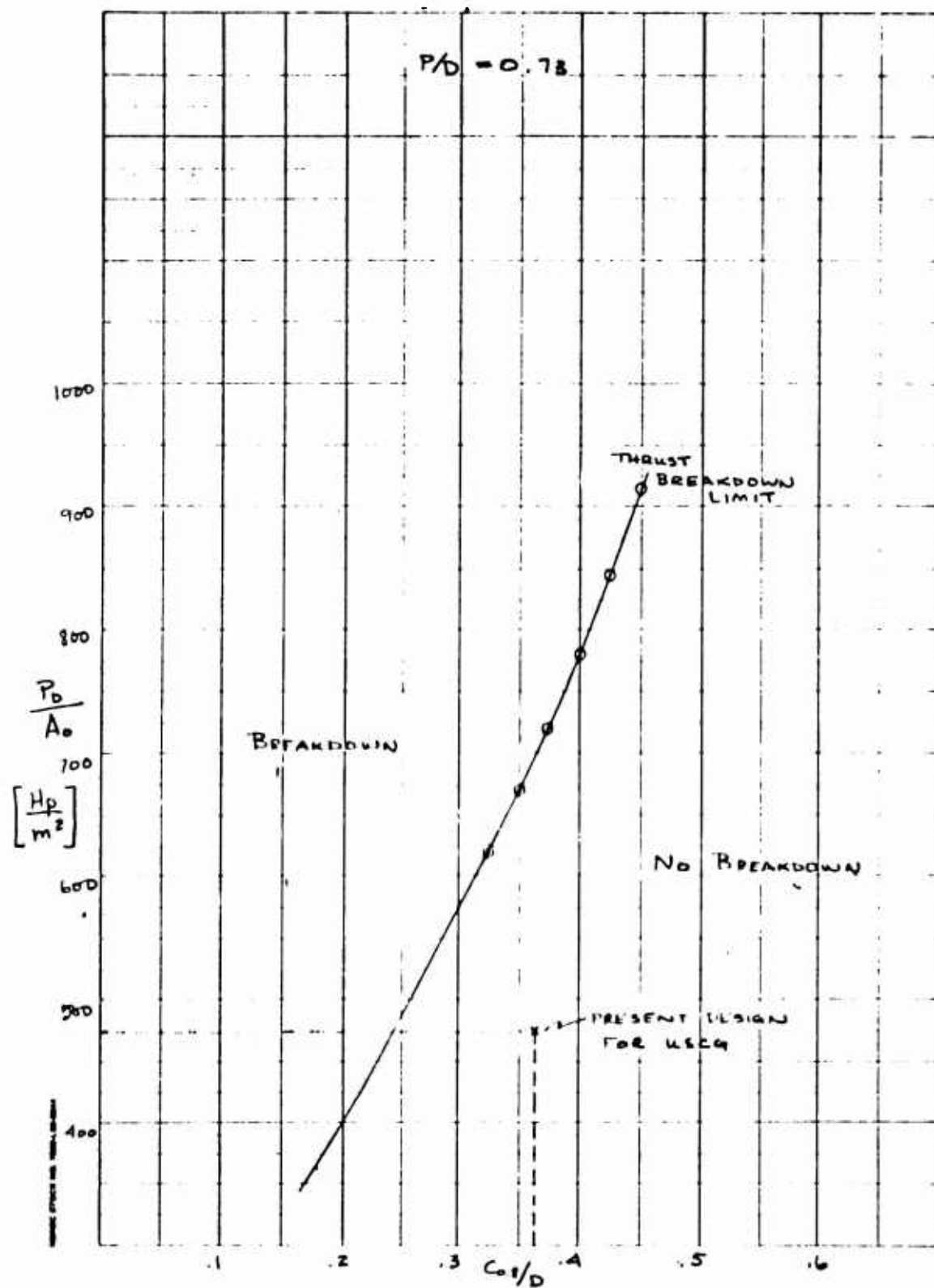


Figure 5 - Self Propulsion Performance of Model 5336 Fitted with Stock Propeller

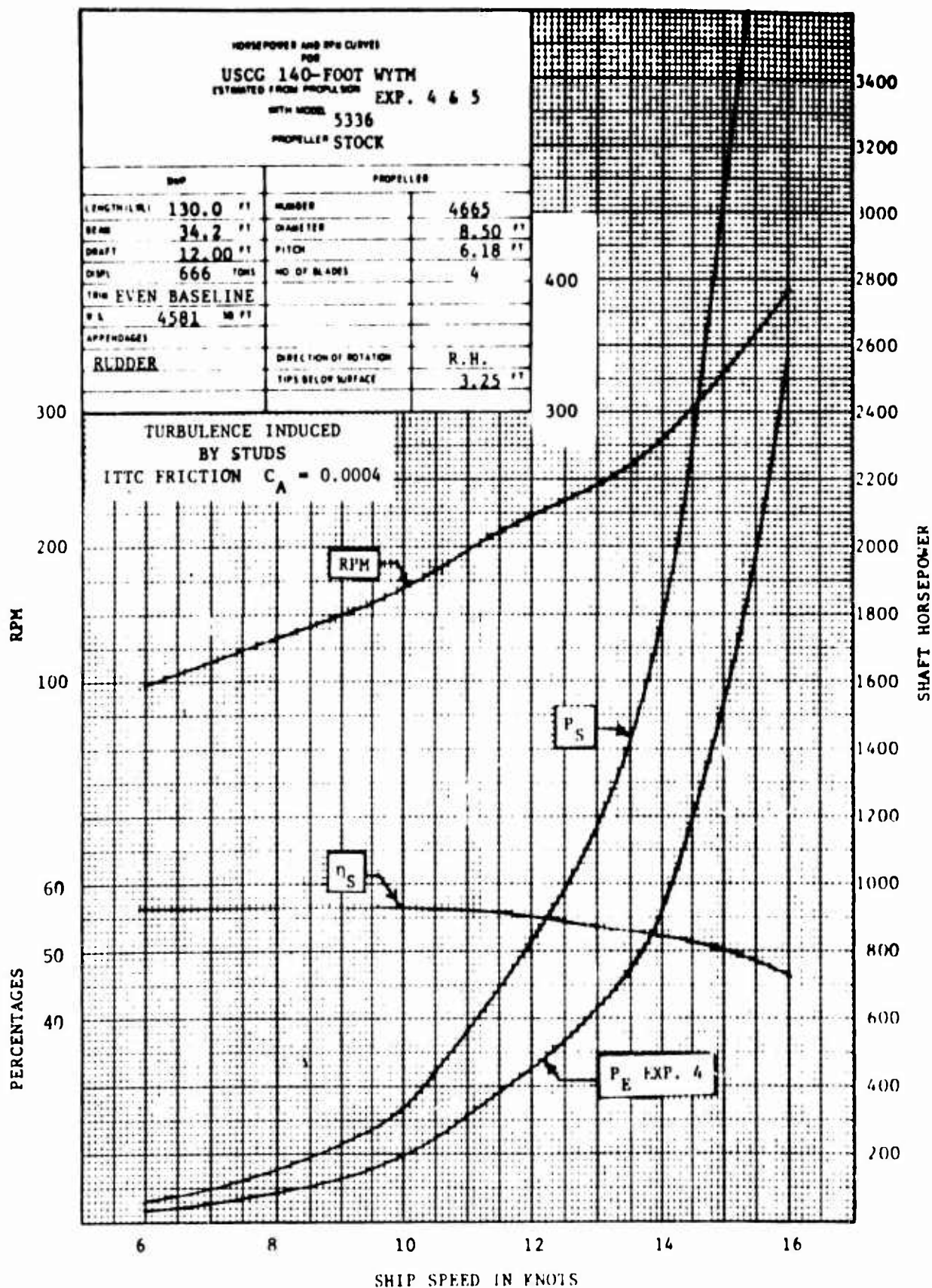


Figure 6 - Series Prediction of Full Power Free Route rpm and Velocity

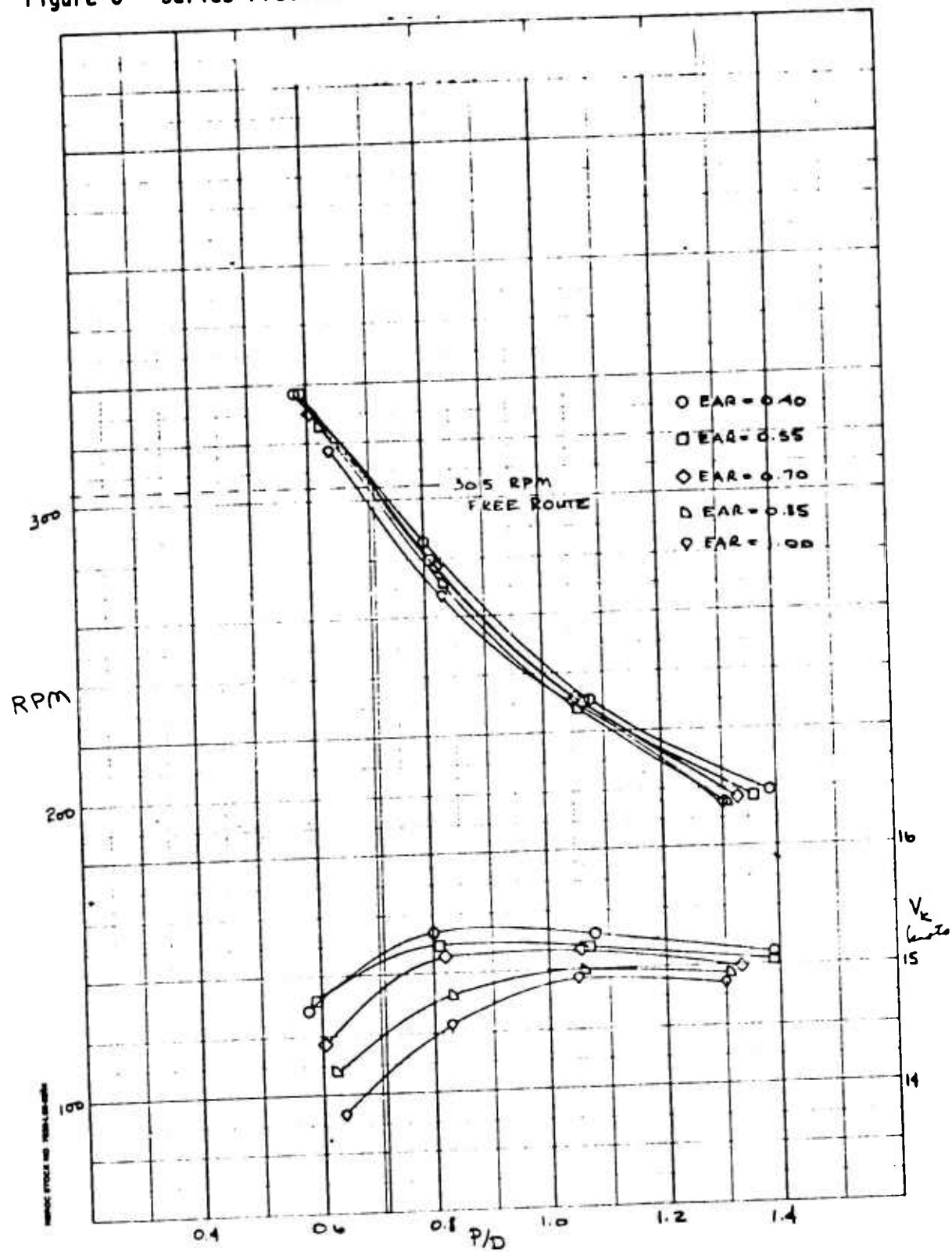
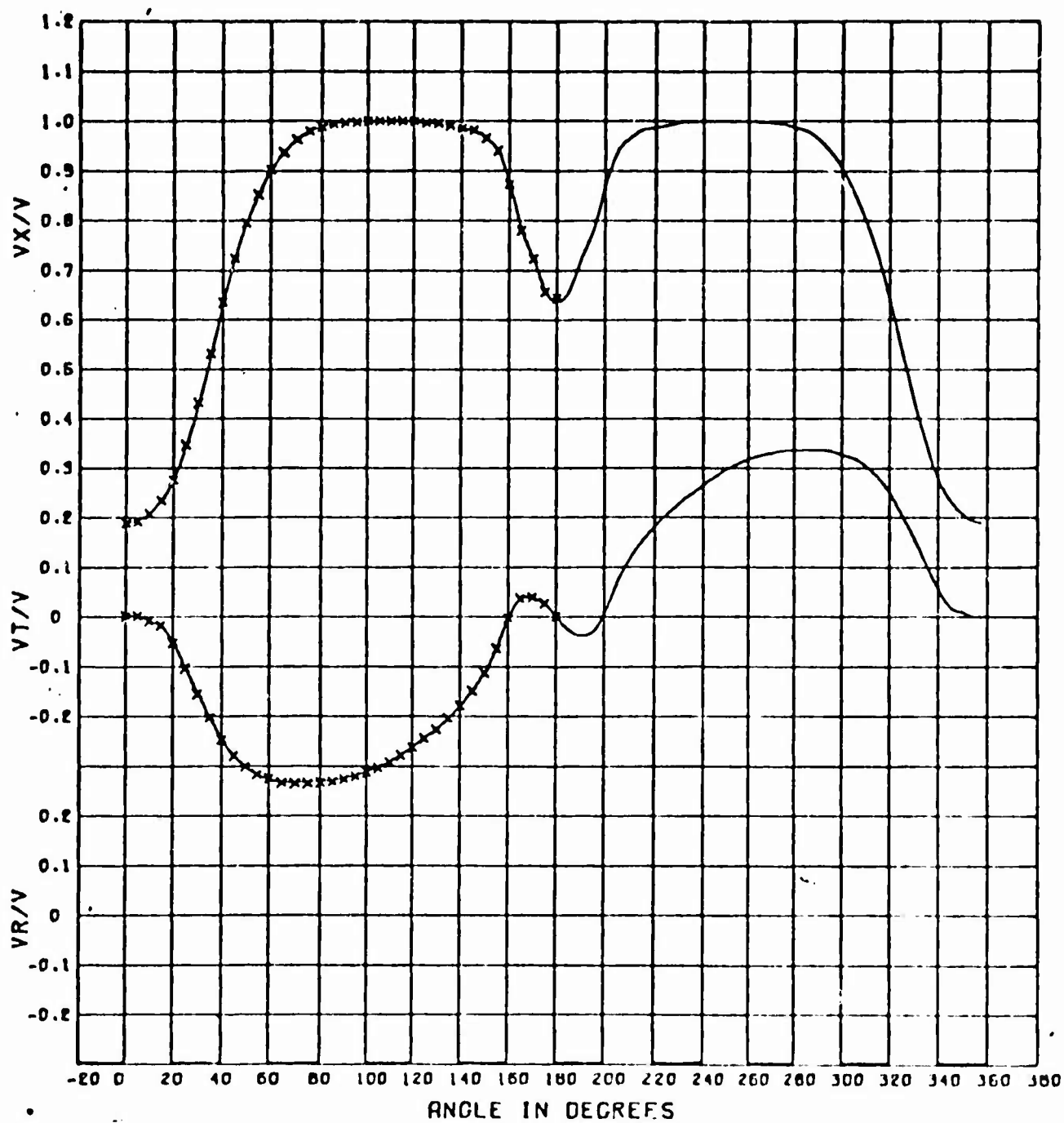
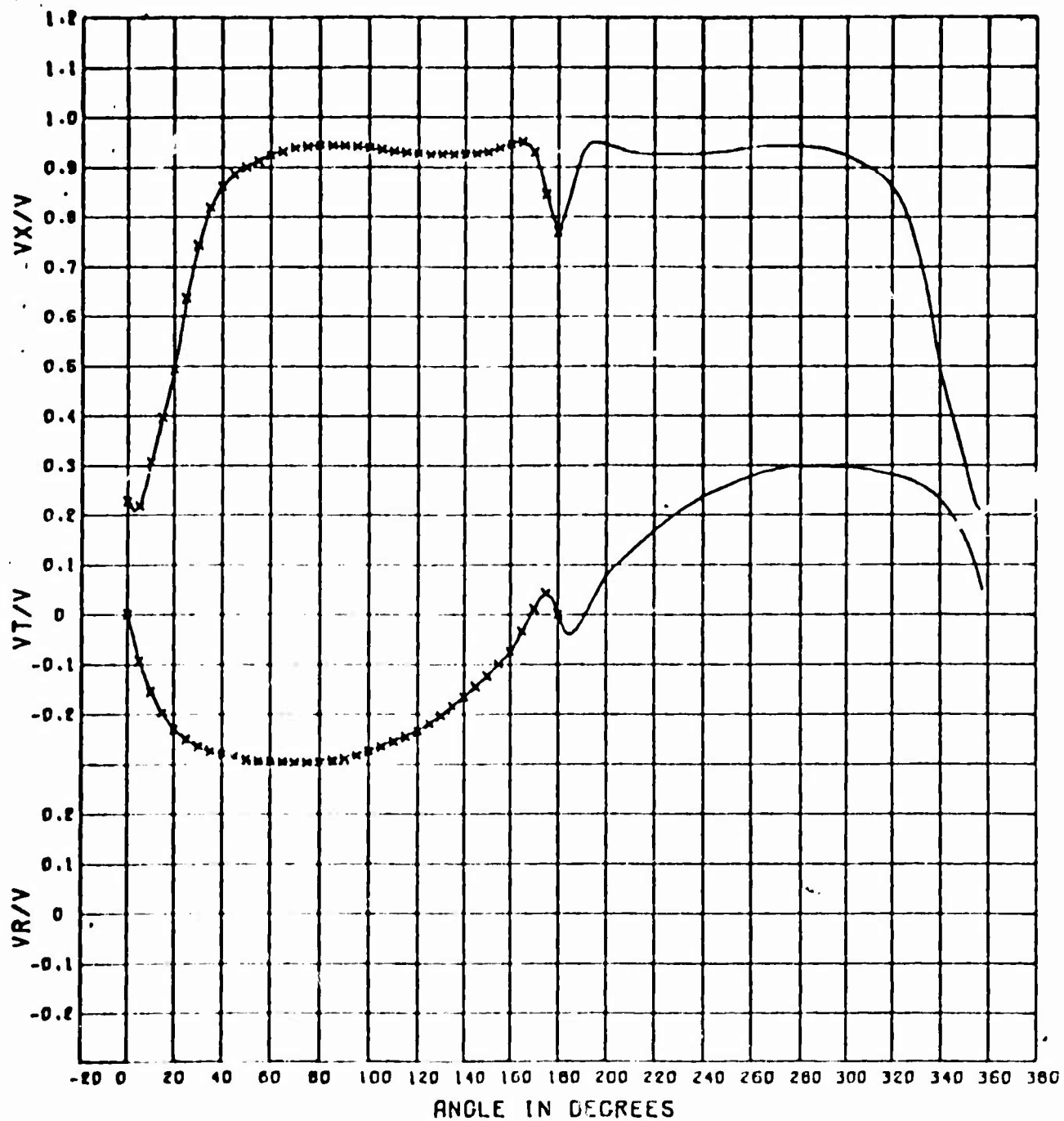


Figure 7 - Wake Survey Velocity Component Ratios at Experimental Rad11



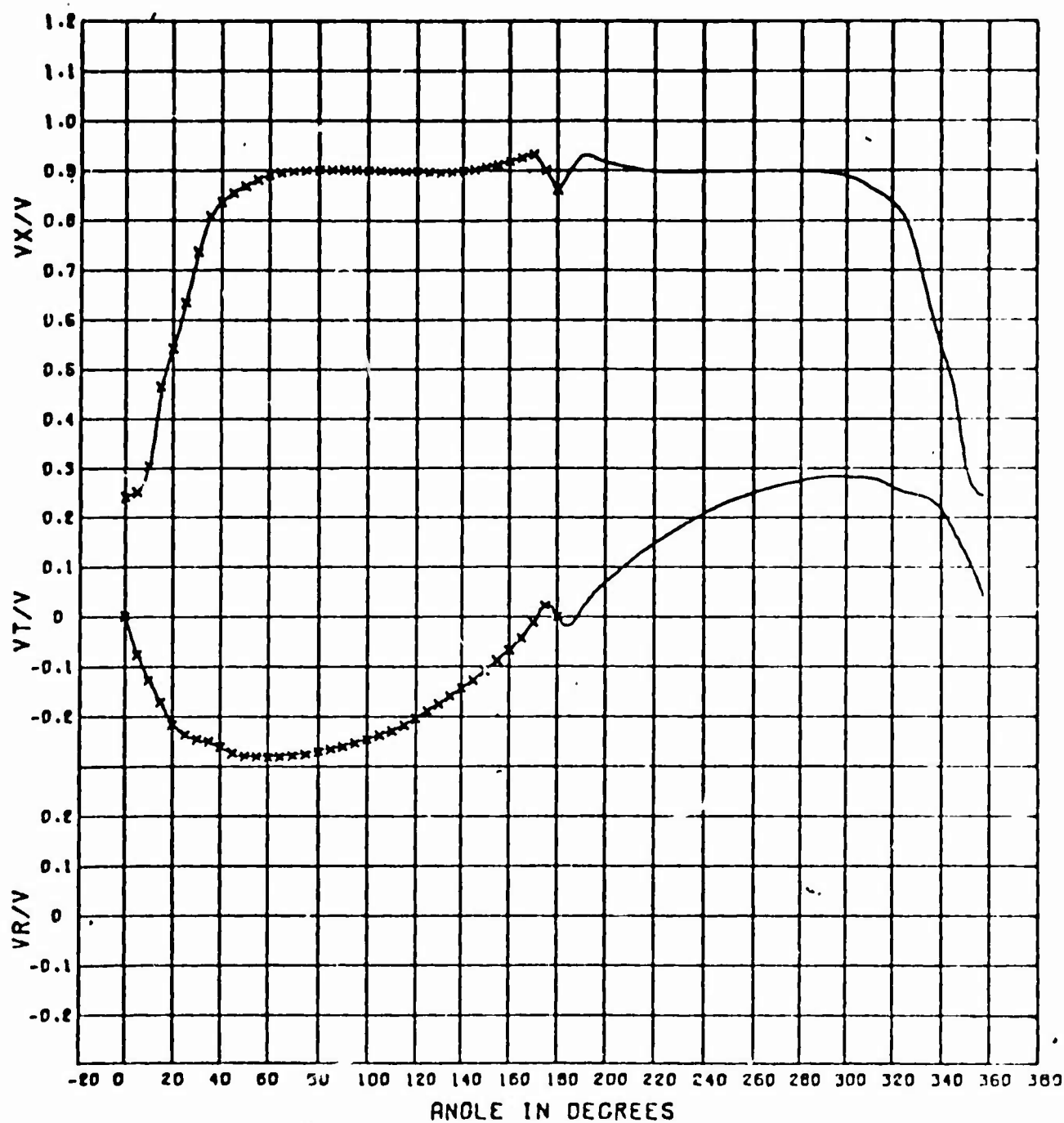
Velocity Component Ratios at the 0.320 Radius Ratio

Figure 7



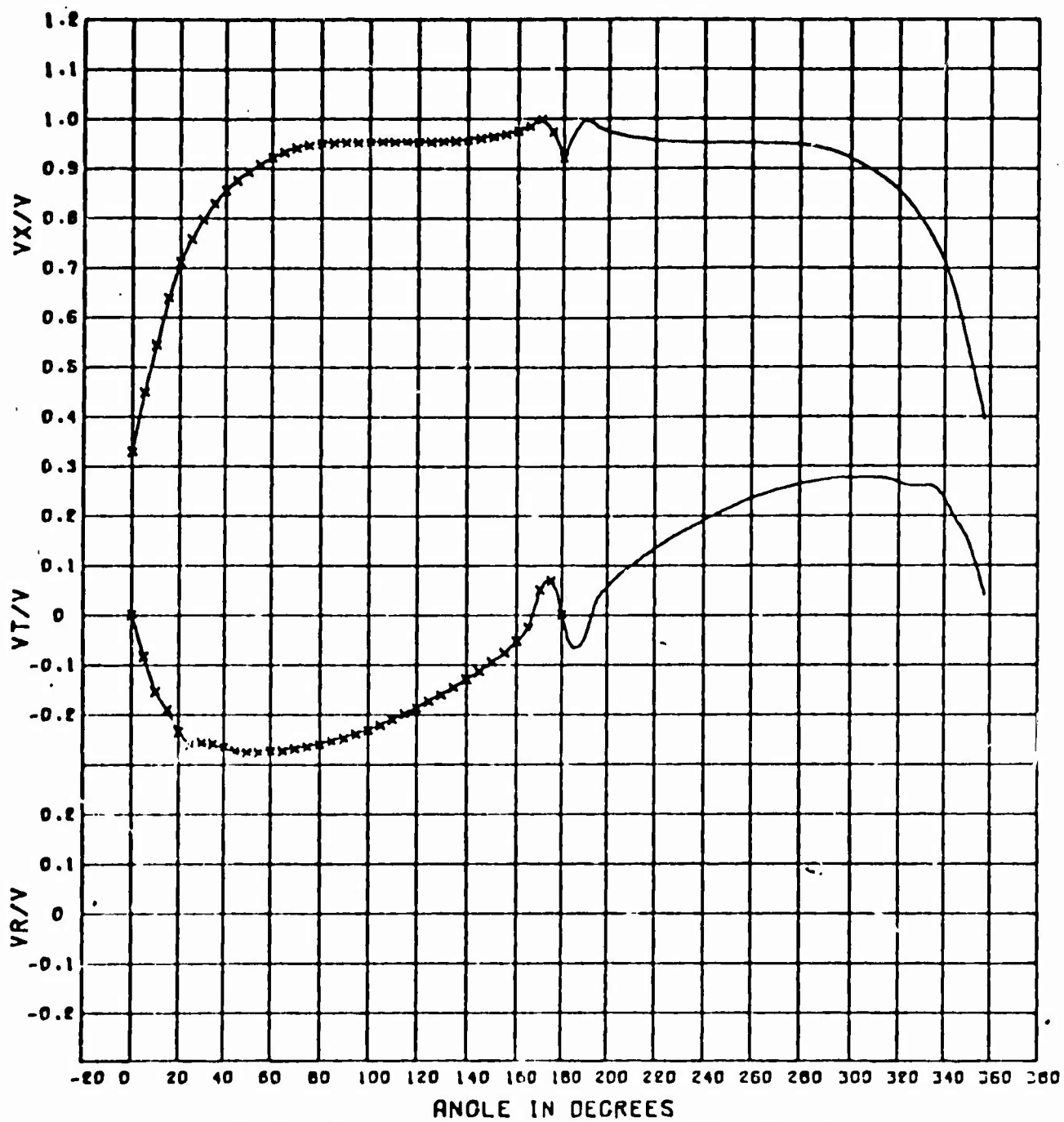
Velocity Component Ratios at the 0.496 Radius Ratio

Figure 7 Continued



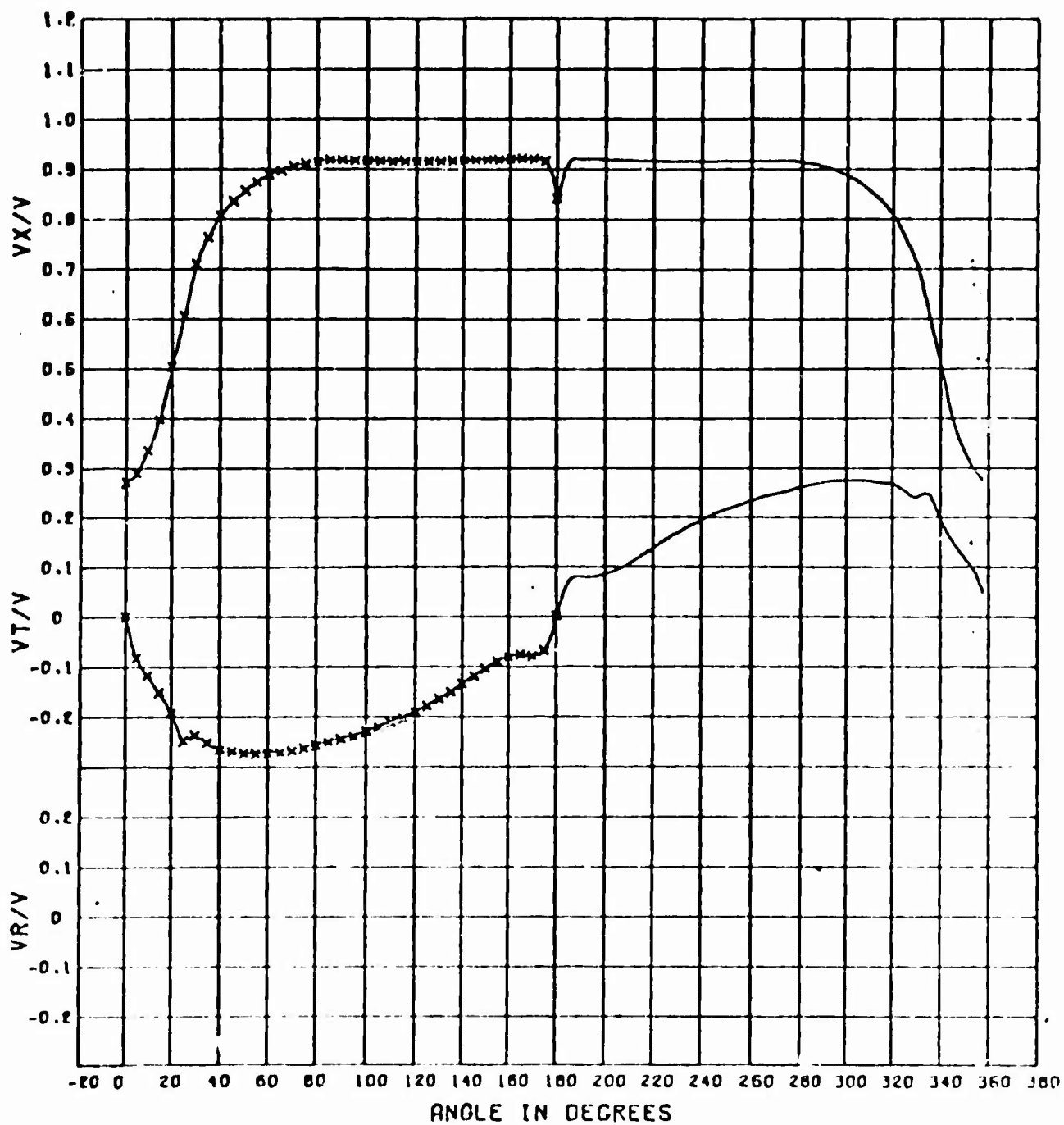
Velocity Component Ratios at the 0.691 Radius Ratio

Figure 7 Continued



Velocity Component Ratios at the 0.907 Radius Ratio

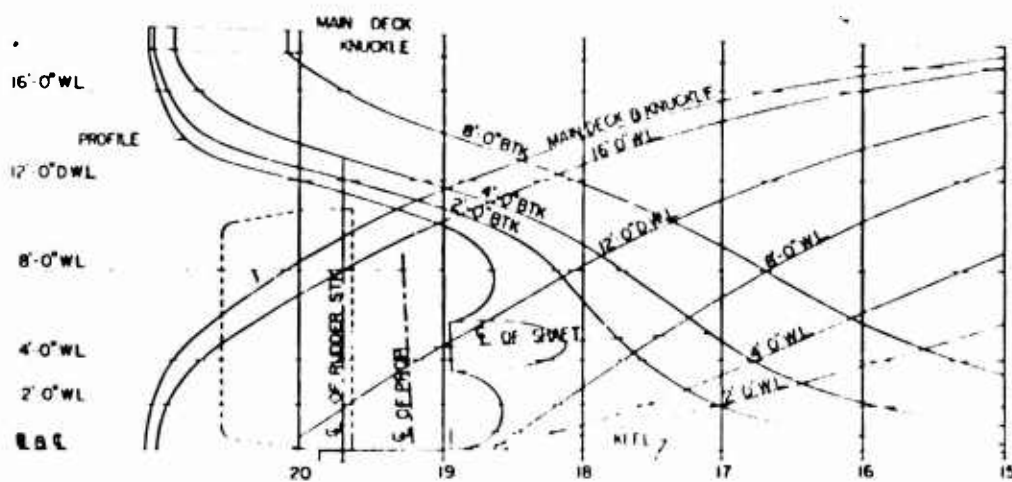
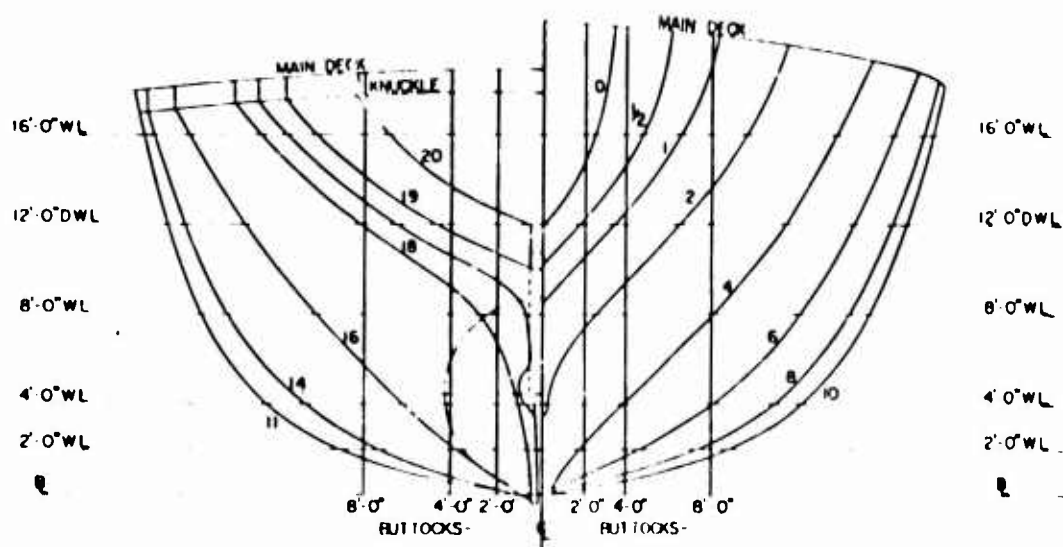
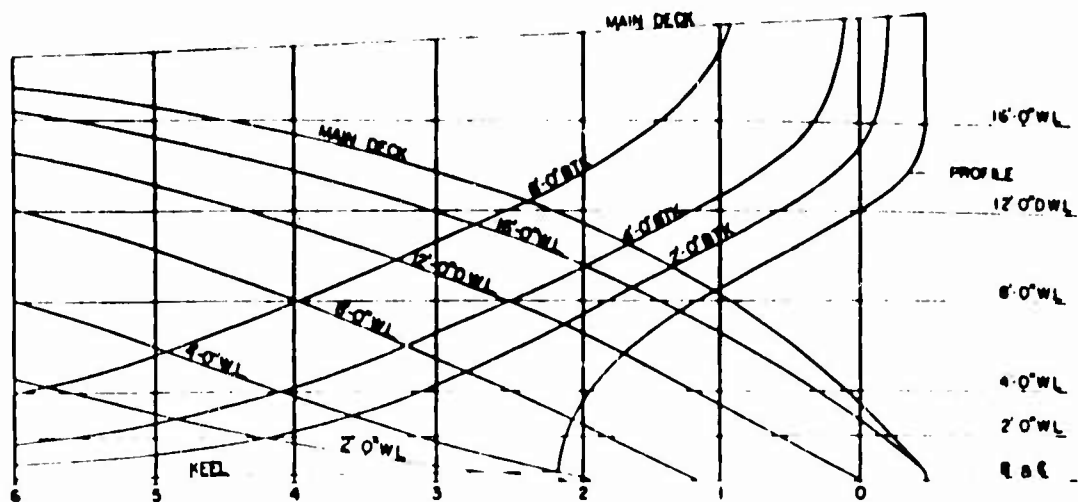
Figure 7 Continued



Velocity Component Ratios at the 1.051 Radius Ratio

Figure 7 Continued





ABBREVIATED LINES AND BODY PLAN  
OF UNITED STATES COAST GUARD 140-FOOT WYTM

Figure 8 - Hull Lines of Model 5336

Figure 9 - Radial Distribution of Thickness

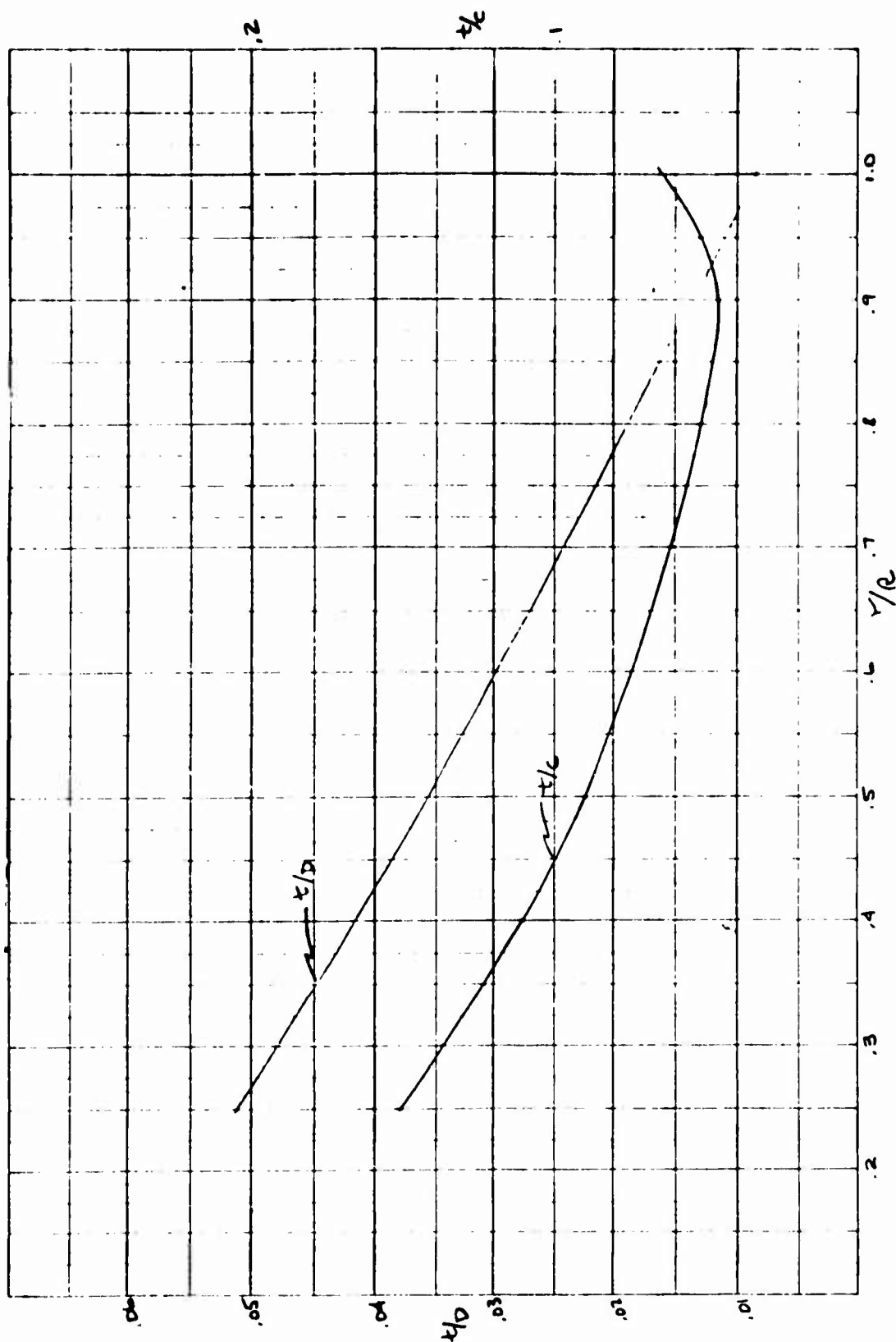
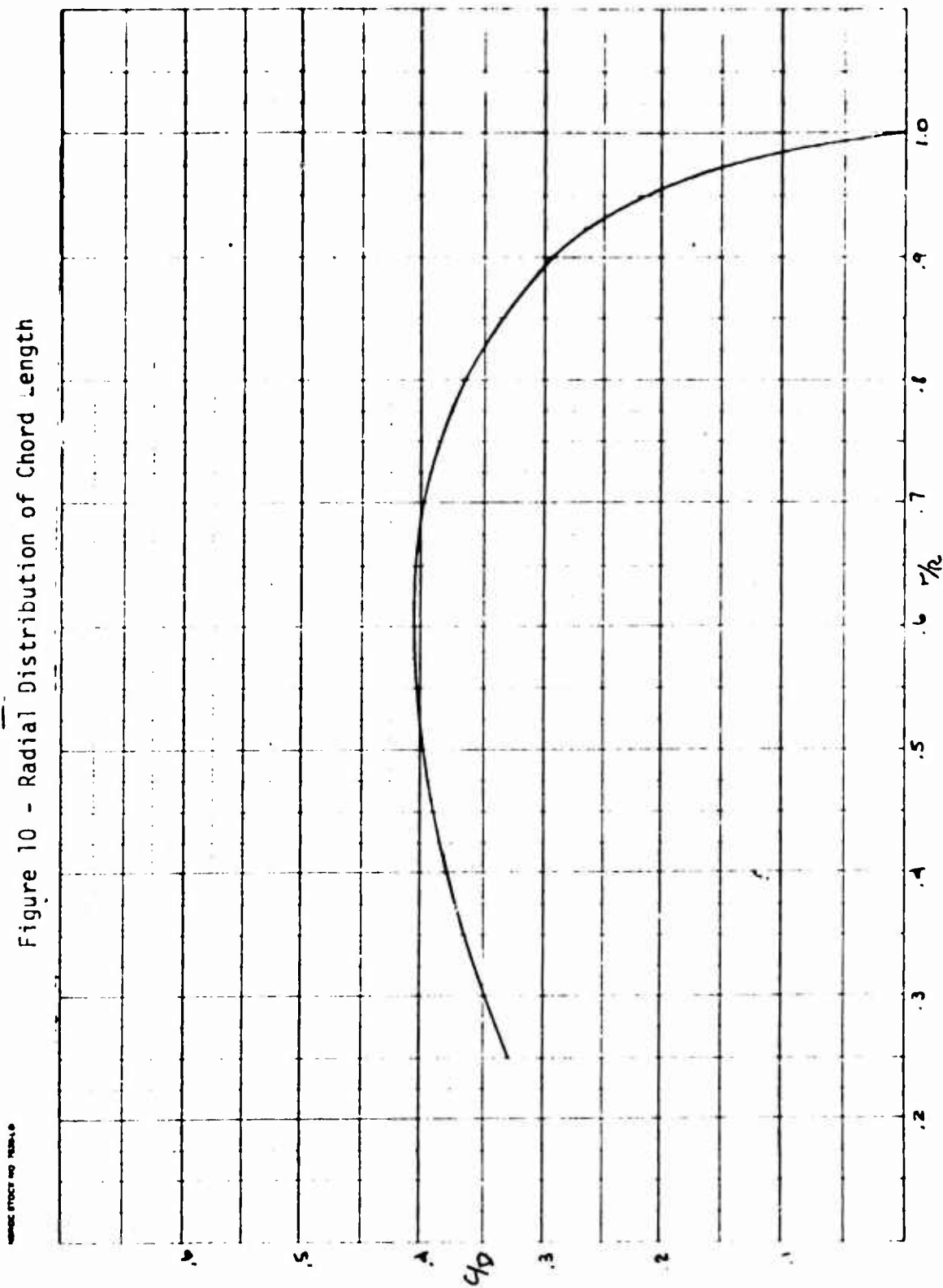


Figure 10 - Radial Distribution of Chord Length



WINDING SPEEDS AND TENSION

Figure 11 - Final Pitch Distribution

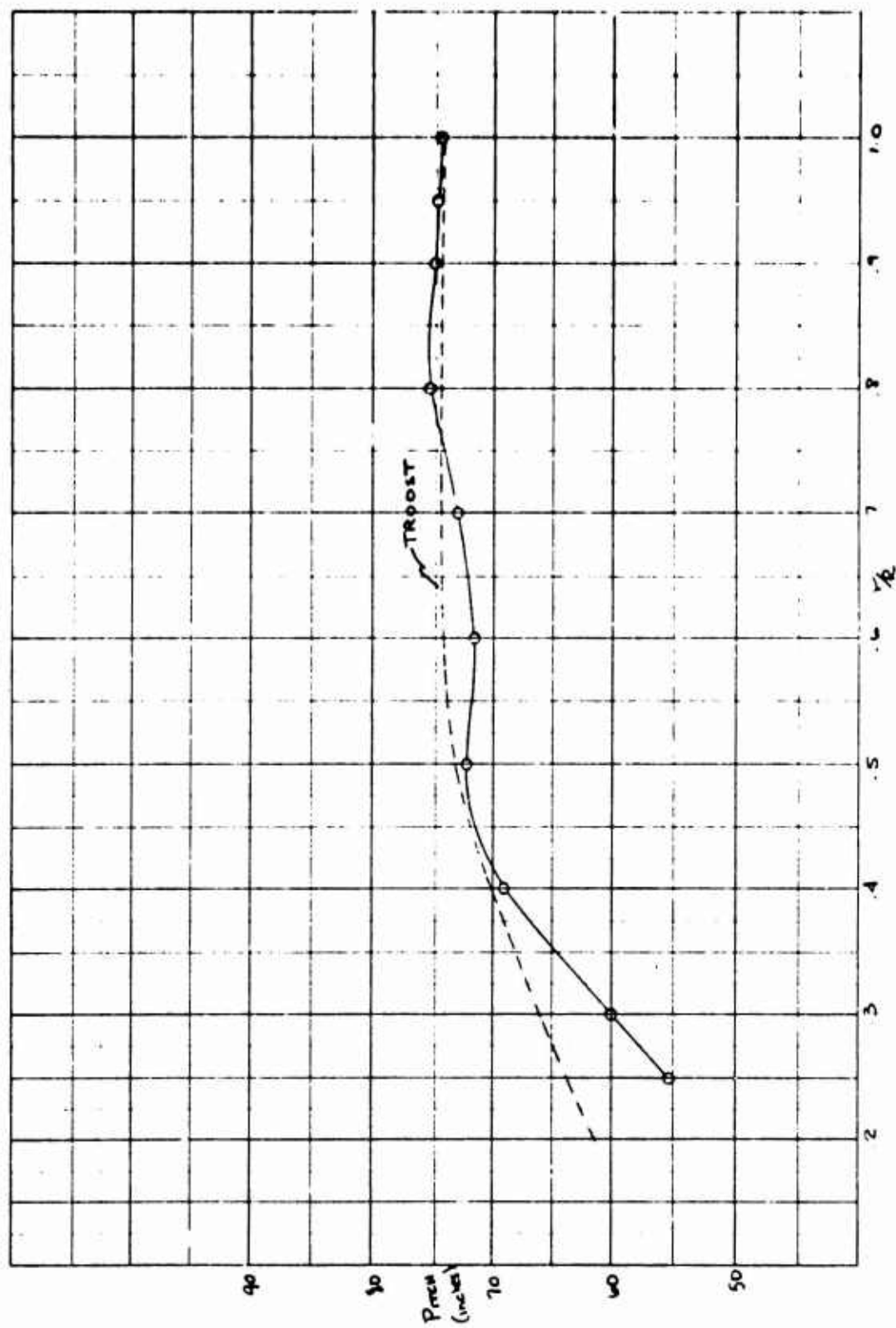
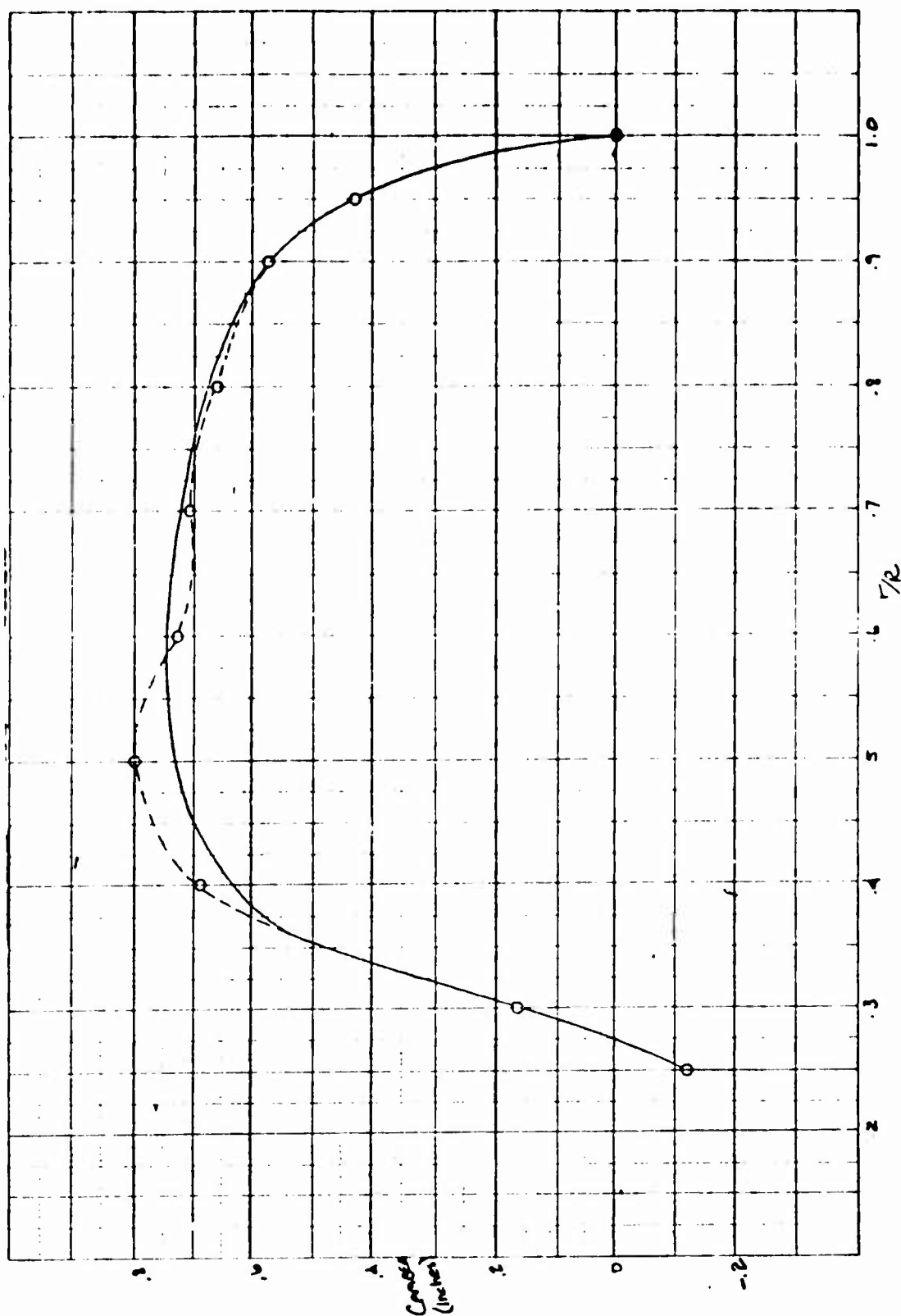


Figure 12 - Final Camber Distribution

WINDUP STITCHES AND TENSION



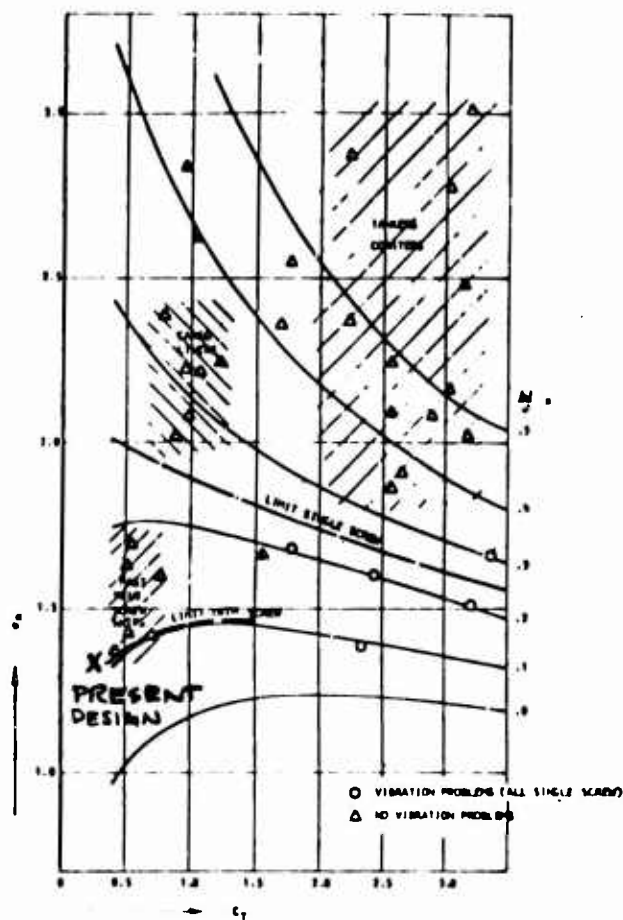


Figure 13 - Limits of Cavitation and Hull-Transmitted Propeller Vibration

TABLE 1

PREDICTIONS OF SHP, RPM AND ALLIED DATA FOR THE 140-FOOT WYTM  
REPRESENTED BY MODEL 5336 WITH PROPELLER 4665

EXPERIMENTS 4 & 5 DISPLACEMENT 666 TONS DRAFT 12.0 FT - EVEN BASELINE  
CORRELATION ALLOWANCE 0.0004 PROPELLER DIAMETER 8.5 FT

$V_S$	$P_E$	$P_S$	RPM	$\eta_S$	$1-W_T$	$J_T$	$1-W_Q$	$1-t$	$\eta_P$	$\eta_H$	$\eta_R$
5.00	20.	35.	81.9	.565	.745	.540	.755	.810	.505	1.090	1.020
6.00	34.	60.	97.9	.565	.740	.540	.750	.810	.505	1.095	1.020
7.00	56.	99.	115.0	.565	.740	.535	.750	.810	.505	1.095	1.015
8.00	88.	156.	132.6	.565	.740	.530	.745	.810	.510	1.100	1.015
9.00	129.	228.	149.9	.565	.735	.525	.740	.810	.510	1.100	1.010
9.50	154.	272.	158.7	.565	.735	.525	.740	.810	.510	1.100	1.010
10.00	189.	334.	169.0	.565	.735	.520	.740	.810	.505	1.100	1.010
10.50	251.	445.	183.9	.565	.740	.500	.750	.810	.505	1.100	1.020
11.00	319.	567.	198.1	.565	.740	.490	.760	.810	.500	1.090	1.030
11.50	389.	697.	211.4	.560	.750	.485	.765	.810	.500	1.085	1.030
12.00	460.	833.	223.5	.550	.750	.480	.770	.810	.500	1.075	1.030
12.50	536.	986.	235.1	.545	.755	.480	.765	.810	.495	1.075	1.020
13.00	611.	1160.	246.4	.535	.755	.475	.760	.810	.495	1.075	1.005
13.50	747.	1410.	261.4	.530	.755	.465	.760	.810	.495	1.070	1.005
14.00	932.	1780.	280.2	.525	.760	.450	.765	.810	.485	1.065	1.010
14.50	1190.	2300.	302.8	.515	.765	.435	.780	.810	.480	1.060	1.020
15.00	1530.	3050.	328.9	.500	.770	.420	.790	.810	.465	1.050	1.020
15.50	1970.	4070.	358.2	.485	.780	.400	.800	.810	.455	1.040	1.020
16.00	2550.	5490.	391.4	.465	.785	.380	.810	.810	.440	1.030	1.020
16.50	3280.	7410.	427.3	.445	.790	.365	.810	.810	.425	1.025	1.015
17.00	4130.	10080.	463.9	.410	.800	.350	.770	.810	.415	1.010	0.980

Table 2  
Wake Survey Analysis for Model 5336

RADIUS	VXBAR	VTBAR	VRBAR	1-WVX	1-WX	BBAR	BPOS	BNEG
.320	.785	0.000	0.000	.770	.793	24.58	11.09	-18.36
.496	.833	0.000	0.000	.804	.817	17.39	4.37	-13.09
.691	.815	0.000	0.000	.817	.825	12.41	2.27	-8.71
.907	.884	0.000	0.000	.830	.836	10.30	1.40	-6.44
1.051	.818	0.000	0.000	.837	.841	8.26	1.40	-5.51
.255	.751	0.000	0.000	0.000	0.000	28.84	16.17	-23.22
.350	.797	0.000	0.000	.778	.799	23.01	9.35	-17.29
.400	.814	0.000	0.000	.789	.806	20.78	7.09	-15.72
.500	.832	0.000	0.000	.806	.819	17.23	4.30	-12.97
.600	.814	0.000	0.000	.813	.823	14.20	3.00	-10.45
.700	.822	0.000	0.000	.814	.822	12.36	2.19	-8.58
.750	.854	0.000	0.000	.818	.825	11.99	1.86	-7.94
.800	.875	0.000	0.000	.824	.830	11.53	1.66	-7.39
.950	.874	0.000	0.000	.842	.847	9.73	1.33	-6.13
1.000	.852	0.000	0.000	.844	.849	9.03	1.34	-5.80



TABLE 3

Stress Levels from Intermediate Design Phase

$\frac{r}{R}$	$\sigma$
0.25	2300
0.35	2000
0.40	1800
0.50	1900
0.60	1550
0.70	1150
0.80	980

TABLE 4

PROPELLED BLADE SECTION DESIGN FOR PRESCRIBED LOAD DISTRIBUTION  
MIT-P90-9

PROPELLED DESIGN FOR USCG ICEBREAKER YUGOAT

DIAMETER-IN 182.00				CHORD LOAD TYPE				69 CHORDWISE PANELS			
HUB DIAM-IN 25.50				ELLIPTICAL				63 RADIAL S-V LINES			
NO. OF BLADES 4				THICKNESS FORT				WITH 2 DEG SPACING			
REVS PER MIN 299.00				NSRDC MOD MACA 66				MAKE ANGLE RATIO=1.0			
SPEED-VS-KTS 14.86								HUB IMAGE IS ABSENT			
R/R0	TAN QS	TAN Q	SL/P0	ST/R0	GAMMA	G	COEFFS	VA/VS	UA/VS	TO/R0	RK/R0
.2763	.5098	.7232	-.3672	.3672	.0139		.035599	.754	.1404	.0992	.0087
.3434	.5711	.8247	-.3623	.3623	.0206		-.033132	.774	.1949	.0929	.0163
.4175	.6265	.8644	-.3473	.3473	.0291		-.020055	.804	.2758	.0889	.0344
.5113	.6782	.8944	-.4018	.4018	.0338		-.070564	.893	.3171	.0698	.0528
.6259	.7296	.9146	-.4050	.4050	.0354		-.000271	.791	.3342	.0578	.0694
.7189	.7727	.9134	-.3938	.3938	.0356		0.032002	.915	.3373	.0464	.0869
.8125	.8110	.8975	-.3521	.3521	.0333		0.000000	.951	.3342	.0368	.1044
.9063	.8515	.8757	-.2908	.2908	.0275		0.000000	.843	.3195	.0263	.1219
.9531	.8735	.8644	-.2031	.2031	.0201		0.000000	.851	.3410	.0212	.1384
1.0000			0.0000	0.0000							

R/R0	P/R0	Z/R0	F/R0	TO/C	ALPHA	R-IN	P-IN	C-IN	FO-IN	TO-IN	R-IN
.2969	.545	.347	.0040	.1429	6.55	15.14	59.62	35.41	.141	5.06	.45
.3438	.613	.362	.0116	.1243	7.24	12.57	64.73	16.95	.429	4.74	.83
.4175	.677	.398	.0270	.1041	7.83	22.31	71.26	19.57	.791	4.12	1.76
.5113	.727	.432	.0447	.0856	7.05	27.09	72.09	40.94	.766	3.51	2.55
.6259	.773	.405	.0713	.0704	6.28	31.88	71.41	41.31	.713	2.91	3.56
.7189	.727	.394	.0776	.0559	5.62	36.66	71.45	40.17	.706	2.37	4.63
.8125	.741	.352	.0767	.0497	5.03	41.44	75.63	35.93	.652	1.84	5.32
.9063	.716	.230	.0793	.0448	4.47	46.22	75.86	29.58	.571	1.33	6.21
.9531	.714	.203	.0254	.0322	4.21	48.61	74.82	20.72	.526	1.00	6.85

TABLE 5

## U.S. Coast Guard Fluctuating Forces

$\bar{T}$	1232.2
$\bar{Q}$	1194.2
$\bar{K}_T \times 10^{-3}$	0.478
$\bar{K}_Q \times 10^{-4}$	0.544
$\bar{F}_V$	194.78
$\bar{F}_H$	383.73
$\bar{M}_V$	1661.8
$\bar{M}_H$	3072.6
$T$	38287.0
$\bar{T}/\bar{T}\%$	3.22

# NTTS

PB-255 798/PAT 17 p PC\$3.50/MF\$3.00

**Thank you for your interest in NTIS. We appreciate your order.**

Sub Total	
Additional Charge	
Enter Grand Total	